47th AIAA/ASME/ASCE/AHS/ASC Structures, Structural Dynamics, and Materials Confere
1 - 4 May 2006, Newport, Rhode Island

AIAA 2006-1828

Second-Order Reliability Formulations in DAKOTA/UQ

M. S. Eldred*
Sandia National Laboratories†, Albuquerque, NM 87185

B.J. Bichon‡
Vanderbilt University, Nashville, TN 37235

Reliability methods are probabilistic algorithms for quantifying the effect of uncertainties in simulation input on response metrics of interest. In particular, they compute approximate response function distribution statistics (probability, reliability, and response levels) based on specified probability distributions for input random variables. In this paper, second-order approaches are explored for both the forward reliability analysis of computing probabilities for specified response levels (the reliability index approach (RIA)) and the inverse reliability analysis of computing response levels for specified probabilities (the performance measure approach (PMA)). These new methods employ second-order Taylor series limit state approximations and second-order probability integrations using analytic, numerical, or quasi-Newton limit state Hessians, and are compared with the traditional second-order reliability method (SORM) as well as two-point limit state approximation methods. These reliability analysis methods are then employed within reliability-based design optimization (RBDO) studies using bi-level and surrogate-based formulations. These RBDO formulations employ analytic sensitivities of response, reliability, and second-order probability levels with respect to design variables that either augment or define distribution parameters for the uncertain variables. Relative performance of these reliability analysis and design algorithms are presented for a number of computational experiments performed using the DAKOTA/UQ software. Results indicate that second-order methods can be both more accurate through improved probability estimates and more efficient through accelerated convergence rates.

I. Introduction

Reliability methods are probabilistic algorithms for quantifying the effect of uncertainties in simulation input on response metrics of interest. In particular, they perform uncertainty quantification (UQ) by computing approximate response function distribution statistics based on specified probability distributions for input random variables. These response statistics include response mean, response standard deviation, and cumulative or complementary cumulative distribution function (CDF/CCDF) response level and probability/reliability level pairings. These methods are often more efficient at computing statistics in the tails of the response distributions (events with low probability) than sampling-based approaches since the number of samples required to resolve a low probability can be prohibitive. Thus, these methods, as their name implies, are often used in a reliability context for assessing the probability of failure of a system when confronted with an uncertain environment.

A number of classical reliability analysis methods are discussed in Ref. 15, including Mean-Value First-Order Second-Moment (MVFOSM), First-Order Reliability Method (FORM), and Second-Order Reliability Method (SORM). More recent methods which seek to improve the efficiency of FORM analysis through limit state approximations include the use of local and multipoint approximations in Advanced Mean Value methods (AMV/AMV+[31]) and Two-point Adaptive Nonlinearity Approximation-based methods (TANA[28,34]), respectively. Each of the FORM-based methods can be employed for "forward" or "inverse" reliability analysis through the reliability index approach (RIA) or performance measure approach (PMA), respectively, as described in Ref. 27.

The capability to assess reliability is broadly useful within a design optimization context, and reliability-based design optimization (RBDO) methods are popular approaches for designing systems while accounting for uncertainty. RBDO approaches may be broadly characterized as bi-level (in which the reliability analysis is nested within the optimization, e.g. Ref. 3), sequential (in which iteration occurs between optimization and reliability analysis, e.g. Refs. 8,33), or unilevel (in which the design and reliability searches are combined into a single optimization, e.g. Ref. 2). Bi-level RBDO methods are simple and general-purpose, but can be computationally demanding. Sequential and unilevel methods seek to reduce computational expense by breaking the nested relationship through the use of iterated or simultaneous approaches.

*Principal Member of Technical Staff, Optimization and Uncertainty Estimation Department, Associate Fellow AIAA.

†Sandia is a multiprogram laboratory operated by Sandia Corporation, a Lockheed-Martin Company, for the United States Department of Energy under Contract DE-AC04-94AL85000.

‡NSF IGERT Fellow, Department of Civil and Environmental Engineering.

In order to provide access to a variety of uncertainty quantification capabilities for analysis of large-scale engineering applications on high-performance parallel computers, the DAKOTA project[10] at Sandia National Laboratories has developed a suite of algorithmic capabilities known as DAKOTA/UQ.[29] This package contains the reliability analysis and RBDO capabilities described in this paper, and is freely available for download worldwide through an open source license.

This paper explores a variety of algorithms for performing reliability analysis. In particular, forward and inverse reliability analyses are performed using multiple limit state approximation, probability integration, Hessian approximation, and optimization algorithm selections. These uncertainty quantification capabilities are then used as a foundation for exploring RBDO formulations. Sections II and III describe these algorithmic components, Section IV provides computational results for four benchmark test problems, and Section V provides concluding remarks.

II. Reliability Method Formulations

A. Mean Value

The Mean Value method (MV, also known as MVFOSM in Ref. 15) is the simplest, least-expensive reliability method because it estimates the response means, response standard deviations, and all CDF/CCDF response-probability-reliability levels from a single evaluation of response functions and their gradients at the uncertain variable means. This approximation can have acceptable accuracy when the response functions are nearly linear and their distributions are approximately Gaussian, but can have poor accuracy in other situations.

With the introduction of second-order limit state information, a second-order mean can be calculated. This is commonly combined with a first-order variance, since second-order variance involves higher order distribution moments (skewness, kurtosis) which are often unavailable. The expressions for approximate response mean μ_g, approximate response standard deviation σ_g, response target to approximate probability/reliability level mapping ($\bar{z} \rightarrow p, \beta$), and probability/reliability target to approximate response level mapping ($\bar{p}, \bar{\beta} \rightarrow z$) are

$$\mu_g = g(\mu_{\mathbf{x}}) + \frac{1}{2} \sum_i \sum_j Cov(i,j) \frac{d^2 g}{dx_i dx_j}(\mu_{\mathbf{x}}) \tag{1}$$

$$\sigma_g = \sum_i \sum_j Cov(i,j) \frac{dg}{dx_i}(\mu_{\mathbf{x}}) \frac{dg}{dx_j}(\mu_{\mathbf{x}}) \tag{2}$$

$$\beta_{cdf} = \frac{\mu_g - \bar{z}}{\sigma_g} \tag{3}$$

$$\beta_{ccdf} = \frac{\bar{z} - \mu_g}{\sigma_g} \tag{4}$$

$$z = \mu_g - \sigma_g \bar{\beta}_{cdf} \tag{5}$$

$$z = \mu_g + \sigma_g \bar{\beta}_{ccdf} \tag{6}$$

respectively, where $\mathbf{x}$ are the uncertain values in the space of the original uncertain variables ("x-space") and $g(\mathbf{x})$ is the limit state function (the response function for which probability-response level pairs are needed). The CDF reliability index β_{cdf}, CCDF reliability index β_{ccdf}, first-order CDF probability $p(g \leq z)$, and first-order CCDF probability $p(g > z)$ are related to one another through

$$p(g \leq z) = \Phi(-\beta_{cdf}) \tag{7}$$

$$p(g > z) = \Phi(-\beta_{ccdf}) \tag{8}$$

$$\beta_{cdf} = -\Phi^{-1}(p(g \leq z)) \tag{9}$$

$$\beta_{ccdf} = -\Phi^{-1}(p(g > z)) \tag{10}$$

$$\beta_{cdf} = -\beta_{ccdf} \tag{11}$$

$$p(g \leq z) = 1 - p(g > z) \tag{12}$$

where $\Phi()$ is the standard normal cumulative distribution function. A common convention in the literature is to define g in such a way that the CDF probability for a response level z of zero (i.e., $p(g \leq 0)$) is the response metric of interest. The formulations in this paper are not restricted to this convention and are designed to support CDF or CCDF mappings for general response, probability, and reliability level sequences.

B. MPP Search Methods

All other reliability methods solve a nonlinear optimization problem to compute a most probable point (MPP) and then integrate about this point to compute probabilities. The MPP search is performed in uncorrelated standard normal space ("u-space") since it simplifies the probability integration: the distance of the MPP from the origin has the meaning of the number of input standard deviations separating the mean response from a particular response threshold. The transformation from correlated non-normal distributions (x-space) to uncorrelated standard normal distributions (u-space) is denoted as $\mathbf{u} = T(\mathbf{x})$ with the reverse transformation denoted as $\mathbf{x} = T^{-1}(\mathbf{u})$. These transformations are nonlinear in general, and possible approaches include the Rosenblatt,[25] Nataf,[7] and Box-Cox[4] transformations. The nonlinear transformations may also be linearized, and common approaches for this include the Rackwitz-Fiessler[23] two-parameter equivalent normal and the Chen-Lind[6] and Wu-Wirsching[30] three-parameter equivalent normals. The results in this paper employ the Nataf nonlinear transformation which occurs in the following two steps. To transform between the original correlated x-space variables and correlated standard normals ("z-space"), the CDF matching condition is used:

$$\Phi(z_i) = F(x_i) \tag{13}$$

where $F()$ is the cumulative distribution function of the original probability distribution. Then, to transform between correlated z-space variables and uncorrelated u-space variables, the Cholesky factor $\mathbf{L}$ of a modified correlation matrix is used:

$$\mathbf{z} = \mathbf{L}\mathbf{u} \tag{14}$$

where the original correlation matrix for non-normals in x-space has been modified for z-space.[7]

The forward reliability analysis algorithm of computing CDF/CCDF probability/reliability levels for specified response levels is called the reliability index approach (RIA), and the inverse reliability analysis algorithm of computing response levels for specified CDF/CCDF probability/reliability levels is called the performance measure approach (PMA).[27] The differences between the RIA and PMA formulations appear in the objective function and equality constraint formulations used in the MPP searches. For RIA, the MPP search for achieving the specified response level $\bar{z}$ is formulated as

$$\begin{aligned} \text{minimize} \quad & \mathbf{u}^T\mathbf{u} \\ \text{subject to} \quad & G(\mathbf{u}) = \bar{z} \end{aligned} \tag{15}$$

and for PMA, the MPP search for achieving the specified reliability/probability level $\bar{\beta}, \bar{p}$ is formulated as

$$\begin{aligned} \text{minimize} \quad & \pm G(\mathbf{u}) \\ \text{subject to} \quad & \mathbf{u}^T\mathbf{u} = \bar{\beta}^2 \end{aligned} \tag{16}$$

where $\mathbf{u}$ is a vector centered at the origin in u-space and $g(\mathbf{x}) \equiv G(\mathbf{u})$ by definition. In the RIA case, the optimal MPP solution $\mathbf{u}^*$ defines the reliability index from $\beta = \pm\|\mathbf{u}^*\|_2$, which in turn defines the CDF/CCDF probabilities (using Eqs. 7-8 in the case of first-order integration). The sign of β is defined by

$$G(\mathbf{u}^*) > G(\mathbf{0}) : \beta_{cdf} < 0, \beta_{ccdf} > 0 \tag{17}$$

$$G(\mathbf{u}^*) < G(\mathbf{0}) : \beta_{cdf} > 0, \beta_{ccdf} < 0 \tag{18}$$

where $G(\mathbf{0})$ is the median limit state response computed at the origin in u-space (where $\beta_{cdf} = \beta_{ccdf} = 0$ and first-order $p(g \leq z) = p(g > z) = 0.5$). In the PMA case, the sign applied to $G(\mathbf{u})$ (equivalent to minimizing or maximizing $G(\mathbf{u})$) is similarly defined by $\bar{\beta}$

$$\bar{\beta}_{cdf} < 0, \bar{\beta}_{ccdf} > 0 : \text{maximize } G(\mathbf{u}) \tag{19}$$

$$\bar{\beta}_{cdf} > 0, \bar{\beta}_{ccdf} < 0 : \text{minimize } G(\mathbf{u}) \tag{20}$$

and the limit state at the MPP ($G(\mathbf{u}^*)$) defines the desired response level result.

When performing PMA with specified $\bar{p}$, one must compute $\bar{\beta}$ to include in Eq. 16. While this is a straightforward one-time calculation for first-order integrations (Eqs. 9-10), the use of second-order integrations complicates matters since the $\bar{\beta}$ corresponding to the prescribed $\bar{p}$ is a function of the Hessian of G (see Eq. 33), which in turn is a function of location in u-space. A generalized reliability index (Eq. 48), which would allow a one-time calculation, may not be used since equality with $\mathbf{u}^T\mathbf{u}$ is not meaningful. The $\bar{\beta}$ target must therefore be updated in Eq. 16 as the minimization progresses (e.g., using Newton's method to solve Eq. 33 for $\bar{\beta}$ given $\bar{p}$ and κ_i). This works best when $\bar{\beta}$ can be fixed during the course of an approximate optimization, such as for the AMV^2+ and TANA methods described in Section II.B.1. For PMA without limit state approximation cycles (i.e., PMA SORM), the constraint must be continually updated and the constraint derivative should include $\nabla_{\mathbf{u}}\bar{\beta}$, which would require third-order information for the limit state to compute derivatives of the principal curvatures. This is impractical, so the PMA SORM constraint derivatives are only approximated analytically or estimated numerically. Potentially for this reason, PMA SORM has not been widely explored in the literature.

1. Limit state approximations

There are a variety of algorithmic variations that can be explored within RIA/PMA reliability analysis. First, one may select among several different limit state approximations that can be used to reduce computational expense during the MPP searches. Local, multipoint, and global approximations of the limit state are possible. Ref. 11 focused on local first-order limit state approximations. This paper will focus on local second-order and multipoint approximations:

1. a single second-order Taylor series per response/reliability/probability level in x-space centered at the uncertain variable means (named AMV^2 due to its extension of the Advanced Mean Value (AMV) method).

$$g(\mathbf{x}) \cong g(\mu_{\mathbf{x}}) + \nabla_{\mathbf{x}} g(\mu_{\mathbf{x}})^T (\mathbf{x} - \mu_{\mathbf{x}}) + \frac{1}{2}(\mathbf{x} - \mu_{\mathbf{x}})^T \nabla^2_{\mathbf{x}} g(\mu_{\mathbf{x}})(\mathbf{x} - \mu_{\mathbf{x}}) \tag{21}$$

2. same as AMV^2, except that the Taylor series is expanded in u-space. This option has been termed the u-space AMV^2 method (note: $\mu_{\mathbf{u}} = T(\mu_{\mathbf{x}})$ and is nonzero in general).

$$G(\mathbf{u}) \cong G(\mu_{\mathbf{u}}) + \nabla_{\mathbf{u}} G(\mu_{\mathbf{u}})^T (\mathbf{u} - \mu_{\mathbf{u}}) + \frac{1}{2}(\mathbf{u} - \mu_{\mathbf{u}})^T \nabla^2_{\mathbf{u}} G(\mu_{\mathbf{u}})(\mathbf{u} - \mu_{\mathbf{u}}) \tag{22}$$

3. an initial second-order Taylor series approximation in x-space at the uncertain variable means, with iterative expansion updates at each MPP estimate ($\mathbf{x}^*$) until the MPP converges (named AMV^2+ due to its extension of the AMV+ method).

$$g(\mathbf{x}) \cong g(\mathbf{x}^*) + \nabla_{\mathbf{x}} g(\mathbf{x}^*)^T (\mathbf{x} - \mathbf{x}^*) + \frac{1}{2}(\mathbf{x} - \mathbf{x}^*)^T \nabla^2_{\mathbf{x}} g(\mathbf{x}^*)(\mathbf{x} - \mathbf{x}^*) \tag{23}$$

4. same as AMV^2+, except that the expansions are performed in u-space. This option has been termed the u-space AMV^2+ method.

$$G(\mathbf{u}) \cong G(\mathbf{u}^*) + \nabla_{\mathbf{u}} G(\mathbf{u}^*)^T (\mathbf{u} - \mathbf{u}^*) + \frac{1}{2}(\mathbf{u} - \mathbf{u}^*)^T \nabla^2_{\mathbf{u}} G(\mathbf{u}^*)(\mathbf{u} - \mathbf{u}^*) \tag{24}$$

5. a multipoint approximation in x-space. This approach involves a Taylor series approximation in intermediate variables where the powers used for the intermediate variables are selected to match information at the current and previous expansion points. Based on the two-point exponential approximation concept (TPEA[12]), the two-point adaptive nonlinearity approximation (TANA-3[34]) approximates the limit state as:

$$g(\mathbf{x}) \cong g(\mathbf{x}_2) + \sum_{i=1}^{n} \frac{\partial g}{\partial x_i}(\mathbf{x}_2) \frac{x_{i,2}^{1-p_i}}{p_i}(x_i^{p_i} - x_{i,2}^{p_i}) + \frac{1}{2}\epsilon(\mathbf{x}) \sum_{i=1}^{n} (x_i^{p_i} - x_{i,2}^{p_i})^2 \tag{25}$$

where n is the number of uncertain variables and:

$$p_i = 1 + \ln\left[\frac{\frac{\partial g}{\partial x_i}(\mathbf{x}_1)}{\frac{\partial g}{\partial x_i}(\mathbf{x}_2)}\right] \Big/ \ln\left[\frac{x_{i,1}}{x_{i,2}}\right] \tag{26}$$

$$\epsilon(\mathbf{x}) = \frac{H}{\sum_{i=1}^{n}(x_i^{p_i} - x_{i,1}^{p_i})^2 + \sum_{i=1}^{n}(x_i^{p_i} - x_{i,2}^{p_i})^2} \tag{27}$$

$$H = 2\left[g(\mathbf{x}_1) - g(\mathbf{x}_2) - \sum_{i=1}^{n} \frac{\partial g}{\partial x_i}(\mathbf{x}_2) \frac{x_{i,2}^{1-p_i}}{p_i}(x_{i,1}^{p_i} - x_{i,2}^{p_i})\right] \tag{28}$$

and $\mathbf{x}_2$ and $\mathbf{x}_1$ are the current and previous MPP estimates in x-space, respectively. Prior to the availability of two MPP estimates, x-space AMV+ is used.

6. a multipoint approximation in u-space. The u-space TANA-3 approximates the limit state as:

$$G(\mathbf{u}) \cong G(\mathbf{u}_2) + \sum_{i=1}^{n} \frac{\partial G}{\partial u_i}(\mathbf{u}_2) \frac{u_{i,2}^{1-p_i}}{p_i}(u_i^{p_i} - u_{i,2}^{p_i}) + \frac{1}{2}\epsilon(\mathbf{u}) \sum_{i=1}^{n} (u_i^{p_i} - u_{i,2}^{p_i})^2 \tag{29}$$

where:

$$p_i = 1 + \ln\left[\frac{\frac{\partial G}{\partial u_i}(\mathbf{u}_1)}{\frac{\partial G}{\partial u_i}(\mathbf{u}_2)}\right] \Big/ \ln\left[\frac{u_{i,1}}{u_{i,2}}\right] \tag{30}$$

$$\epsilon(\mathbf{u}) = \frac{H}{\sum_{i=1}^{n}(u_i^{p_i} - u_{i,1}^{p_i})^2 + \sum_{i=1}^{n}(u_i^{p_i} - u_{i,2}^{p_i})^2} \quad (31)$$

$$H = 2\left[G(\mathbf{u}_1) - G(\mathbf{u}_2) - \sum_{i=1}^{n}\frac{\partial G}{\partial u_i}(\mathbf{u}_2)\frac{u_{i,2}^{1-p_i}}{p_i}(u_{i,1}^{p_i} - u_{i,2}^{p_i})\right] \quad (32)$$

and $\mathbf{u}_2$ and $\mathbf{u}_1$ are the current and previous MPP estimates in u-space, respectively. Prior to the availability of two MPP estimates, u-space AMV+ is used.

7. the MPP search on the original response functions without the use of any approximations.

The Hessian matrices in AMV^2 and AMV^2+ may be available analytically, estimated numerically, or approximated through quasi-Newton updates. The quasi-Newton variant of AMV^2+ is conceptually similar to TANA in that both approximate curvature based on a sequence of gradient evaluations. TANA estimates curvature by matching values and gradients at two points and includes it through the use of exponential intermediate variables and a single-valued diagonal Hessian approximation. Quasi-Newton AMV^2+ accumulates curvature over a sequence of points and then uses it directly in a second-order series expansion. Therefore, these methods may be expected to exhibit similar performance.

The selection between x-space or u-space for performing approximations depends on where the approximation will be more accurate, since this will result in more accurate MPP estimates (AMV^2) or faster convergence (AMV^2+, TANA). Since this relative accuracy depends on the forms of the limit state $g(x)$ and the transformation $T(x)$ and is therefore application dependent in general, DAKOTA/UQ supports both options. A concern with approximation-based iterative search methods (i.e., AMV^2+ and TANA) is the robustness of their convergence to the MPP. It is possible for the MPP iterates to oscillate or even diverge. However, to date, this occurrence has been relatively rare, and DAKOTA/UQ contains checks that monitor for this behavior. Another concern with TANA is numerical safeguarding. First, there is the possibility of raising negative x_i or u_i values to nonintegral p_i exponents in Eqs. 25, 27-29, and 31-32. This is particularly likely for u-space. Safeguarding techniques include the use of linear bounds scaling for each x_i or u_i, offseting negative x_i or u_i, or promotion of p_i to integral values for negative x_i or u_i. In numerical experimentation, the offset approach has been the most effective in retaining the desired data matches without overly inflating the p_i exponents. Second, there are a number of potential numerical difficulties with the logarithm ratios in Eqs. 26 and 30. In this case, a safeguarding strategy is to revert to either the linear ($p_i = 1$) or reciprocal ($p_i = -1$) approximation based on which approximation has lower error in $\frac{\partial g}{\partial x_i}(\mathbf{x}_1)$ or $\frac{\partial G}{\partial u_i}(\mathbf{u}_1)$.

2. Probability integrations

The second algorithmic variation involves the integration approach for computing probabilities at the MPP, which can be selected to be first-order (Eqs. 7-8) or second-order integration. Second-order integration involves applying a curvature correction.[5,17,18] Breitung applies a correction based on asymptotic analysis:[5]

$$p = \Phi(-\beta_p)\prod_{i=1}^{n-1}\frac{1}{\sqrt{1+\beta_p\kappa_i}} \quad (33)$$

where κ_i are the principal curvatures of the limit state function (the eigenvalues of an orthonormal transformation of $\nabla^2_{\mathbf{u}}G$, taken positive for a convex limit state) and $\beta_p \geq 0$ (select CDF or CCDF probability correction to obtain correct sign for β_p). An alternate correction in Ref. 17 is consistent in the asymptotic regime ($\beta_p \to \infty$) but does not collapse to first-order integration for $\beta_p = 0$:

$$p = \Phi(-\beta_p)\prod_{i=1}^{n-1}\frac{1}{\sqrt{1+\psi(-\beta_p)\kappa_i}} \quad (34)$$

where $\psi() = \frac{\phi()}{\Phi()}$ and $\phi()$ is the standard normal density function. Ref. 18 applies further corrections to Eq. 34 based on point concentration methods.

To invert a second-order integration and compute β_p given p and κ_i (e.g., for second-order PMA as described in Section II.B, Newton's method can be applied using the recursion

$$\beta_p^{k+1} = \beta_p^k - \frac{f(\beta_p)}{df/d\beta} \quad (35)$$

in order to drive $f(\beta_p) \to 0$, where for Breitung's correction (Eq. 33)

$$f(\beta_p) = p\prod_{i=1}^{n-1}\sqrt{1+\beta_p\kappa_i} - \Phi(-\beta_p) \quad (36)$$

$$\frac{df}{d\beta} = p\sum_{i=1}^{n-1}\left(\frac{\kappa_i}{2\sqrt{1+\beta_p\kappa_i}}\prod_{\substack{j=1\\ j\neq i}}^{n-1}\sqrt{1+\beta_p\kappa_j}\right)+\phi(-\beta_p) \tag{37}$$

An initial guess of $\beta_p^0 = -\Phi^{-1}(p)$ is used (again, select CDF or CCDF probability to obtain nonnegative β_p^0), and a backtracking line search is employed to provide globalization of Newton's method by verifying reduction in $f(\beta_p)$.

Combining the no-approximation option of the MPP search with first-order and second-order integration approaches results in the traditional first-order and second-order reliability methods (FORM and SORM). Additional probability integration approaches can involve importance sampling in the vicinity of the MPP,[17,32] but are outside the scope of this paper. While second-order integrations could be performed anywhere a limit state Hessian has been computed, the additional computational effort is most warranted for fully converged MPPs from AMV^2+, TANA, and SORM, and is of reduced value for MVSOSM or AMV^2. The results in this paper follow this guidance in that all probabilities presented for AMV^2+, TANA, and SORM are second-order, and all probabilities presented for MVSOSM and AMV^2 are first-order.

3. Hessian approximations

To use a second-order Taylor series or a second-order integration when second-order information ($\nabla^2_{\mathbf{x}}g$, $\nabla^2_{\mathbf{u}}G$, and/or κ) is not directly available, one can estimate the missing information using finite differences or approximate it through use of quasi-Newton approximations. These procedures will often be needed to make second-order approaches practical for engineering applications.

In the finite difference case, numerical Hessians are commonly computed using either first-order forward differences of gradients using

$$\nabla^2 g(\mathbf{x}) \cong \frac{\nabla g(\mathbf{x}+h\mathbf{e}_i)-\nabla g(\mathbf{x})}{h} \tag{38}$$

to estimate the i^{th} Hessian column when gradients are analytically available, or second-order differences of function values using

$$\nabla^2 g(\mathbf{x}) \cong \frac{g(\mathbf{x}+h\mathbf{e}_i+h\mathbf{e}_j)-g(\mathbf{x}+h\mathbf{e}_i-h\mathbf{e}_j)-g(\mathbf{x}-h\mathbf{e}_i+h\mathbf{e}_j)+g(\mathbf{x}-h\mathbf{e}_i-h\mathbf{e}_j)}{4h^2} \tag{39}$$

to estimate the ij^{th} Hessian term when gradients are not directly available. This approach has the advantage of locally-accurate Hessians for each point of interest (which can lead to quadratic convergence rates in discrete Newton methods), but has the disadvantage that numerically estimating each of the matrix terms can be expensive.

Quasi-Newton approximations, on the other hand, do not reevaluate all of the second-order information for every point of interest. Rather, they accumulate approximate curvature information over time using secant updates. Since they utilize the existing gradient evaluations, they do not require any additional function evaluations for evaluating the Hessian terms. The quasi-Newton approximations of interest include the Broyden-Fletcher-Goldfarb-Shanno (BFGS) update

$$\mathbf{B}_{k+1} = \mathbf{B}_k - \frac{\mathbf{B}_k\mathbf{s}_k\mathbf{s}_k^T\mathbf{B}_k}{\mathbf{s}_k^T\mathbf{B}_k\mathbf{s}_k} + \frac{\mathbf{y}_k\mathbf{y}_k^T}{\mathbf{y}_k^T\mathbf{s}_k} \tag{40}$$

which yields a sequence of symmetric positive definite Hessian approximations, and the Symmetric Rank 1 (SR1) update

$$\mathbf{B}_{k+1} = \mathbf{B}_k + \frac{(\mathbf{y}_k-\mathbf{B}_k\mathbf{s}_k)(\mathbf{y}_k-\mathbf{B}_k\mathbf{s}_k)^T}{(\mathbf{y}_k-\mathbf{B}_k\mathbf{s}_k)^T\mathbf{s}_k} \tag{41}$$

which yields a sequence of symmetric, potentially indefinite, Hessian approximations. $\mathbf{B}_k$ is the k^{th} approximation to the Hessian $\nabla^2 g$, $\mathbf{s}_k = \mathbf{x}_{k+1}-\mathbf{x}_k$ is the step and $\mathbf{y}_k = \nabla g_{k+1} - \nabla g_k$ is the corresponding yield in the gradients. The selection of BFGS versus SR1 involves the importance of retaining positive definiteness in the Hessian approximations; if the procedure does not require it, then the SR1 update can be more accurate if the true Hessian is not positive definite. In both cases, an initial scaling of $\mathbf{y}_k^T\mathbf{y}_k/\mathbf{y}_k^T\mathbf{s}_k\mathbf{I}$ is used for $\mathbf{B}_0$ prior to the first update[22] and safeguarding against numerical failures is required. A common safeguard for BFGS is to use the damped BFGS approach when the curvature condition $\mathbf{y}_k^T\mathbf{s}_k > 0$ is (nearly) violated.[22] However, while this is appropriate for Newton-like optimization algorithms, numerical experience indicates that the damped BFGS update can degrade performance when the steps generated are not generally Newton-like, resulting in frequent violations of the curvature condition. A more effective approach in this case is to ignore the curvature condition and simply safeguard against small denominators in Eq. 40, skipping the update if $|\mathbf{y}_k^T\mathbf{s}_k| < 10^{-6}\mathbf{s}_k^T\mathbf{B}_k\mathbf{s}_k$. In the SR1 case, the update is similarly skipped when the denominator in Eq. 41 is small, in particular when $|(\mathbf{y}_k-\mathbf{B}_k\mathbf{s}_k)^T\mathbf{s}_k| < 10^{-6}||\mathbf{s}_k||_2||\mathbf{y}_k-\mathbf{B}_k\mathbf{s}_k||_2$.

4. Optimization algorithms

The next algorithmic variation involves the optimization algorithm selection for solving Eqs. 15 and 16. The Hasofer-Lind Rackwitz-Fissler (HL-RF) algorithm[15] is a classical approach that has been broadly applied. It is a Newton-based approach lacking line search/trust region globalization, and is generally regarded as computationally efficient but occasionally unreliable. DAKOTA/UQ takes the approach of employing robust, general-purpose optimization algorithms with provable convergence properties. This paper employs the sequential quadratic programming (SQP) and nonlinear interior-point (NIP) optimization algorithms from the NPSOL[13] and OPT++[21] libraries, respectively.

5. Warm Starting of MPP Searches

The final algorithmic variation involves the use of warm starting approaches for improving computational efficiency. Ref. 11 describes the acceleration of MPP searches through warm starting with approximate iteration increment, with $z/p/\beta$ level increment, and with design variable increment. Warm started data includes the expansion point and associated response values and the MPP optimizer initial guess. Projections are used when an increment in $z/p/\beta$ level or design variables occurs. Warm starts were consistently effective in Ref. 11 and are adopted for all computational experiments in this paper.

III. Reliability-Based Design Optimization

Reliability-based design optimization (RBDO) methods are used to perform design optimization accounting for reliability metrics. The reliability analysis capabilities described in Section II provide a rich foundation for exploring a variety of RBDO formulations. This paper will present second-order methods for bi-level and sequential RBDO.

A. Bi-level RBDO

The simplest and most direct RBDO approach is the bi-level approach in which a full reliability analysis is performed for every optimization function evaluation. This involves a nesting of two distinct levels of optimization within each other, one at the design level and one at the MPP search level.

Since an RBDO problem will typically specify both the $\bar{z}$ level and the $\bar{p}/\bar{\beta}$ level, one can use either the RIA or the PMA formulation for the UQ portion and then constrain the result in the design optimization portion. In particular, RIA reliability analysis maps $\bar{z}$ to p/β, so RIA RBDO constrains p/β:

$$\begin{aligned} \text{minimize} \quad & f \\ \text{subject to} \quad & \beta \geq \bar{\beta} \\ \text{or} \quad & p \leq \bar{p} \end{aligned} \tag{42}$$

And PMA reliability analysis maps $\bar{p}/\bar{\beta}$ to z, so PMA RBDO constrains z:

$$\begin{aligned} \text{minimize} \quad & f \\ \text{subject to} \quad & z \geq \bar{z} \end{aligned} \tag{43}$$

where $z \geq \bar{z}$ is used as the RBDO constraint for a cumulative failure probability (failure defined as $z \leq \bar{z}$) but $z \leq \bar{z}$ would be used as the RBDO constraint for a complementary cumulative failure probability (failure defined as $z \geq \bar{z}$). It is worth noting that DAKOTA is not limited to these types of inequality-constrained RBDO formulations; rather, they are convenient examples. DAKOTA supports general optimization under uncertainty mappings[9] which allow flexible use of statistics within multiple objectives, inequality constraints, and equality constraints.

An important performance enhancement for bi-level methods is the use of sensitivity analysis to analytically compute the design gradients of probability, reliability, and response levels. When design variables are separate from the uncertain variables (i.e., they are not distribution parameters), then the following first-order expressions may be used:[3, 16, 19]

$$\nabla_{\mathbf{d}} z = \nabla_{\mathbf{d}} g \tag{44}$$

$$\nabla_{\mathbf{d}} \beta_{cdf} = \frac{1}{\| \nabla_{\mathbf{u}} G \|} \nabla_{\mathbf{d}} g \tag{45}$$

$$\nabla_{\mathbf{d}} p_{cdf} = -\phi(-\beta_{cdf}) \nabla_{\mathbf{d}} \beta_{cdf} \tag{46}$$

where it is evident from Eqs. 11-12 that $\nabla_{\mathbf{d}}\beta_{ccdf} = -\nabla_{\mathbf{d}}\beta_{cdf}$ and $\nabla_{\mathbf{d}}p_{ccdf} = -\nabla_{\mathbf{d}}p_{cdf}$. In the case of second-order integrations, Eq. 46 must be expanded to include the curvature correction. For Breitung's correction (Eq. 33),

$$\nabla_{\mathbf{d}}p_{cdf} = \left[\Phi(-\beta_p)\sum_{i=1}^{n-1}\left(\frac{-\kappa_i}{2(1+\beta_p\kappa_i)^{\frac{3}{2}}}\prod_{\substack{j=1\\j\neq i}}^{n-1}\frac{1}{\sqrt{1+\beta_p\kappa_j}}\right) - \phi(-\beta_p)\prod_{i=1}^{n-1}\frac{1}{\sqrt{1+\beta_p\kappa_i}}\right]\nabla_{\mathbf{d}}\beta_{cdf} \tag{47}$$

where $\nabla_{\mathbf{d}}\kappa_i$ has been neglected and $\beta_p \geq 0$ (see Section II.B.2). Other approaches assume the curvature correction is nearly independent of the design variables,[24] which is equivalent to neglecting the first term in Eq. 47.

To capture second-order probability estimates within an RIA RBDO formulation using well-behaved β constraints, a generalized reliability index can be introduced where, similar to Eq. 9,

$$\beta^*_{cdf} = -\Phi^{-1}(p_{cdf}) \tag{48}$$

for second-order p_{cdf}. This reliability index is no longer equivalent to the magnitude of $\mathbf{u}$, but rather is a convenience metric for capturing the effect of more accurate probability estimates. The corresponding generalized reliability index sensitivity, similar to Eq. 46, is

$$\nabla_{\mathbf{d}}\beta^*_{cdf} = -\frac{1}{\phi(-\beta^*_{cdf})}\nabla_{\mathbf{d}}p_{cdf} \tag{49}$$

where $\nabla_{\mathbf{d}}p_{cdf}$ is defined from Eq. 47. Even when $\nabla_{\mathbf{d}}g$ is estimated numerically, Eqs. 44-49 can be used to avoid numerical differencing across full reliability analyses.

When the design variables are distribution parameters of the uncertain variables, $\nabla_{\mathbf{d}}g$ is expanded with the chain rule and Eqs. 44 and 45 become

$$\nabla_{\mathbf{d}}z = \nabla_{\mathbf{d}}\mathbf{x}\nabla_{\mathbf{x}}g \tag{50}$$

$$\nabla_{\mathbf{d}}\beta_{cdf} = \frac{1}{\parallel \nabla_{\mathbf{u}}G \parallel}\nabla_{\mathbf{d}}\mathbf{x}\nabla_{\mathbf{x}}g \tag{51}$$

where the design Jacobian of the transformation ($\nabla_{\mathbf{d}}\mathbf{x}$) may be obtained analytically for uncorrelated $\mathbf{x}$ or semi-analytically for correlated $\mathbf{x}$ ($\nabla_{\mathbf{d}}\mathbf{L}$ is evaluated numerically) by differentiating Eqs. 13 and 14 with respect to the distribution parameters. Eqs. 46-49 remain the same as before. For this design variable case, all required information for the sensitivities is available from the MPP search.

Since Eqs. 44-51 are derived using the Karush-Kuhn-Tucker optimality conditions for a converged MPP, they are appropriate for RBDO using AMV^2+, TANA, and SORM, but not for RBDO using MVSOSM or AMV^2.

B. Sequential/Surrogate-based RBDO

An alternative RBDO approach is the sequential approach, in which additional efficiency is sought through breaking the nested relationship of the MPP and design searches. The general concept is to iterate between optimization and uncertainty quantification, updating the optimization goals based on the most recent probabilistic assessment results. This update may be based on safety factors[33] or other approximations.[8]

A particularly effective approach for updating the optimization goals is to use the $p/\beta/z$ sensitivity analysis of Eqs. 44-51 in combination with local surrogate models.[35] In Ref. 11, first-order Taylor series approximations were explored, and in this paper, second-order Taylor series approximations are investigated. In both cases, a trust-region model management framework[14] is used to adaptively manage the extent of the approximations and ensure convergence of the RBDO process. Surrogate models are used for both the objective function and the constraints, although the use of constraint surrogates alone is sufficient to remove the nesting.

In particular, RIA trust-region surrogate-based RBDO employs surrogate models of f and p/β within a trust region Δ^k centered at $\mathbf{d}_c$:

$$\begin{aligned}
\text{minimize} \quad & f(\mathbf{d}_c) + \nabla_{\mathbf{d}}f(\mathbf{d}_c)^T(\mathbf{d}-\mathbf{d}_c) + \tfrac{1}{2}(\mathbf{d}-\mathbf{d}_c)^T\nabla^2_{\mathbf{d}}f(\mathbf{d}_c)(\mathbf{d}-\mathbf{d}_c)\\
\text{subject to} \quad & \beta(\mathbf{d}_c) + \nabla_{\mathbf{d}}\beta(\mathbf{d}_c)^T(\mathbf{d}-\mathbf{d}_c) + \tfrac{1}{2}(\mathbf{d}-\mathbf{d}_c)^T\nabla^2_{\mathbf{d}}\beta(\mathbf{d}_c)(\mathbf{d}-\mathbf{d}_c) \geq \bar{\beta}\\
\text{or} \quad & p(\mathbf{d}_c) + \nabla_{\mathbf{d}}p(\mathbf{d}_c)^T(\mathbf{d}-\mathbf{d}_c) + \tfrac{1}{2}(\mathbf{d}-\mathbf{d}_c)^T\nabla^2_{\mathbf{d}}p(\mathbf{d}_c)(\mathbf{d}-\mathbf{d}_c) \leq \bar{p}\\
& \parallel \mathbf{d}-\mathbf{d}_c \parallel_\infty \leq \Delta^k
\end{aligned} \tag{52}$$

and PMA trust-region surrogate-based RBDO employs surrogate models of f and z within a trust region Δ^k centered at $\mathbf{d}_c$:

$$\begin{aligned} \text{minimize} \quad & f(\mathbf{d}_c) + \nabla_{\mathbf{d}} f(\mathbf{d}_c)^T(\mathbf{d}-\mathbf{d}_c) + \tfrac{1}{2}(\mathbf{d}-\mathbf{d}_c)^T\nabla^2_{\mathbf{d}} f(\mathbf{d}_c)(\mathbf{d}-\mathbf{d}_c) \\ \text{subject to} \quad & z(\mathbf{d}_c) + \nabla_{\mathbf{d}} z(\mathbf{d}_c)^T(\mathbf{d}-\mathbf{d}_c) + \tfrac{1}{2}(\mathbf{d}-\mathbf{d}_c)^T\nabla^2_{\mathbf{d}} z(\mathbf{d}_c)(\mathbf{d}-\mathbf{d}_c) \geq \bar{z} \\ & \| \mathbf{d}-\mathbf{d}_c \|_\infty \leq \Delta^k \end{aligned} \tag{53}$$

where the sense of the z constraint may vary as described previously. The second-order information in Eqs. 52-53 will typically be approximated with quasi-Newton updates.

IV. Computational Experiments

The algorithmic variations of interest in second-order reliability analysis include the limit state approximation approaches (MVSOSM, x-/u-space AMV^2, x-/u-space AMV^2+, x-/u-space TANA, and SORM), integration approaches (first-/second-order), Hessian calculation approaches (analytic, finite difference, BFGS, or SR1), and MPP optimization algorithm selections (SQP or NIP). RBDO algorithmic variations of interest include use of bi-level or sequential approaches, use of RIA or PMA formulations for the underlying UQ, and the specific $z/p/\beta$ mappings that are employed. Relative performance of these algorithmic variations will be presented in this section for a number of computational experiments performed using the DAKOTA/UQ software.[29] DAKOTA/UQ is the uncertainty quantification component of DAKOTA,[10] an open-source software framework for design and performance analysis of computational models on high performance computers. Deployment of these algorithms to realistic engineering problems is explored separately in Ref. 1 through the probabilistic analysis and design of micro-electro-mechanical systems (MEMS).

A. Lognormal ratio

This test problem has a limit state function defined by the ratio of two lognormally-distributed random variables.

$$g(\mathbf{x}) = \frac{x_1}{x_2} \tag{54}$$

The distributions for both x_1 and x_2 are Lognormal(1, 0.5) with a correlation coefficient between the two variables of 0.3.

1. Uncertainty quantification

For RIA, 24 response levels (.4, .5, .55, .6, .65, .7, .75, .8, .85, .9, 1, 1.05, 1.15, 1.2, 1.25, 1.3, 1.35, 1.4, 1.5, 1.55, 1.6, 1.65, 1.7, and 1.75) are mapped into the corresponding cumulative probability levels using first-order (for MVSOSM and AMV^2) or second-order (for AMV^2+, TANA, and SORM) integrations. For PMA, these 24 probability levels (the fully converged first-order or second-order results from RIA FORM/SORM) are mapped back into the original response levels. As described in Section II.B, second-order PMA with prescribed probability levels involves the use of updating schemes for $\bar{\beta}$ in Eq. 16 and is the more challenging PMA case. Tables 1 and 3 show the computational results for each of the primary RIA and PMA method variants using analytic limit state gradients and Hessians, and Tables 2 and 4 show the computational results for RIA and PMA with AMV^2+ using either numerical Hessians or quasi-Newton Hessian updates. Duplicate function evaluations (detected by DAKOTA's evaluation cache) are not included in the totals, an AMV^2+/TANA convergence tolerance of $\| \mathbf{u}^{(k+1)} - \mathbf{u}^{(k)} \|_2 < 10^{-4}$ is used to give comparable accuracy to the SORM converged results, and an asterisk ($*$) is used to indicate when one or more levels fails to converge to full accuracy. The RIA p error norms and PMA z error norms are measured relative to the corresponding fully-converged FORM or SORM results. That is, the inherent reliability analysis errors (e.g., RIA SORM p error norm of 0.05469 and PMA SORM z error norm of 0.03775) relative to a Latin Hypercube reference solution of 10^6 samples are not included in order to avoid obscuring the relative errors. Figure 1 overlays the computed CDF values for each of the eight primary method variants corresponding to Tables 1 and 3 as well as the Latin Hypercube reference solution (any unconverged CDF values, as denoted by $*$ in the tables, are omitted for clarity). Figure 2 displays the convergence rates for different x-space MPP search methods in converging to the first RIA or PMA level.

It is evident that, relative to the fully-converged SORM results, MVSOSM has relatively poor accuracy across the full range. AMV^2 is reasonably accurate over the full range, although with mild offsets from the target response levels, and AMV^2+ and TANA have full accuracy with reductions in expense (on average) relative to SORM. For this problem, AMV^2+ with analytic Hessians and TANA are comparable, and x-space AMV^2+ is the top performer. When approximating Hessians for AMV^2+, numerical Hessians are accurate although too expensive to be competitive, whereas SR1 quasi-Newton updates are accurate, competitive, and superior to BFGS updates (it is more important to accurately

Table 1. RIA results for lognormal ratio problem using analytic Hessians.

RIA Approach	SQP Function Evals (val/grad/Hessian)	NIP Function Evals (val/grad/Hessian)	CDF p Error Norm	Target z Offset Norm
MVSOSM	1 (1/1/1)	1 (1/1/1)	0.3683	0.0
x-space AMV^2	26 (26/1/1)	26 (26/1/1)	0.01369	0.1353
u-space AMV^2	26* (26/1/1)	26 (26/1/1)	0.02438	0.1049
x-space AMV^2+	70 (70/69/69)	75 (75/74/74)	0.0	0.0
u-space AMV^2+	102 (102/101/101)	108 (108/107/107)	0.0	0.0
x-space TANA	83 (83/82/24)	85 (85/84/24)	0.0	0.0
u-space TANA	86 (86/85/24)	86 (86/85/24)	0.0	0.0
SORM	330 (306/305/24)	123 (99/98/24)	0.0	0.0

Table 2. RIA results for lognormal ratio problem using numerical Hessians (NH) and quasi-Hessians (QH).

RIA Approach	SQP Function Evals (val/grad/Hessian)	NIP Function Evals (val/grad/Hessian)	CDF p Error Norm	Target z Offset Norm
x-space AMV^2+ NH	217 (73/216/0)	223 (75/222/0)	1.657e-6	0.0
u-space AMV^2+ NH	304 (102/303/0)	322 (108/321/0)	1.806e-6	0.0
x-space AMV^2+ QH SR1	78 (78/77/0)	84 (84/83/0)	0.001063	0.0
u-space AMV^2+ QH SR1	98 (98/97/0)	105 (105/104/0)	5.731e-7	0.0
x-space AMV^2+ QH BFGS	147 (147/146/0)	123 (123/122/0)	1.073e-4	0.0
u-space AMV^2+ QH BFGS	163 (163/162/0)	139 (139/138/0)	4.530e-5	0.0

Table 3. PMA results for lognormal ratio problem using analytic Hessians.

PMA Approach	SQP Function Evals (val/grad/Hessian)	NIP Function Evals (val/grad/Hessian)	CDF z Error Norm	Target p Offset Norm
MVSOSM	1 (1/1/1)	1 (1/1/1)	0.6277	0.0
x-space AMV^2	26 (26/1/1)	26 (26/1/1)	0.4024	0.008609
u-space AMV^2	26 (26/1/1)	26 (26/1/1)	0.04915	0.008423
x-space AMV^2+	77 (77/76/76)	80 (80/79/79)	0.0	0.0
u-space AMV^2+	92 (92/91/91)	112 (112/111/111)	0.0	0.0
x-space TANA	135* (135/134/24)	135* (135/134/24)	0.01869	0.007251
u-space TANA	111* (111/110/24)	115* (115/114/24)	0.01869	0.007251
SORM	698* (698/697/697)	106* (106/105/105)	0.01902	0.007701

Table 4. PMA results for lognormal ratio problem using numerical Hessians (NH) and quasi-Hessians (QH).

PMA Approach	SQP Function Evals (val/grad/Hessian)	NIP Function Evals (val/grad/Hessian)	CDF z Error Norm	Target p Offset Norm
x-space AMV^2+ NH	229 (77/228/0)	238 (80/237/0)	7.460e-6	4.716e-6
u-space AMV^2+ NH	274 (92/273/0)	334 (112/333/0)	1.012e-5	6.627e-6
x-space AMV^2+ QH SR1	143 (143/142/0)	146 (146/145/0)	0.002518	3.604e-4
u-space AMV^2+ QH SR1	178 (178/177/0)	167 (167/166/0)	0.001099	7.716e-4
x-space AMV^2+ QH BFGS	169 (169/168/0)	172 (172/171/0)	0.1470	0.09317
u-space AMV^2+ QH BFGS	208 (208/207/0)	219 (219/218/0)	0.4932	0.4104

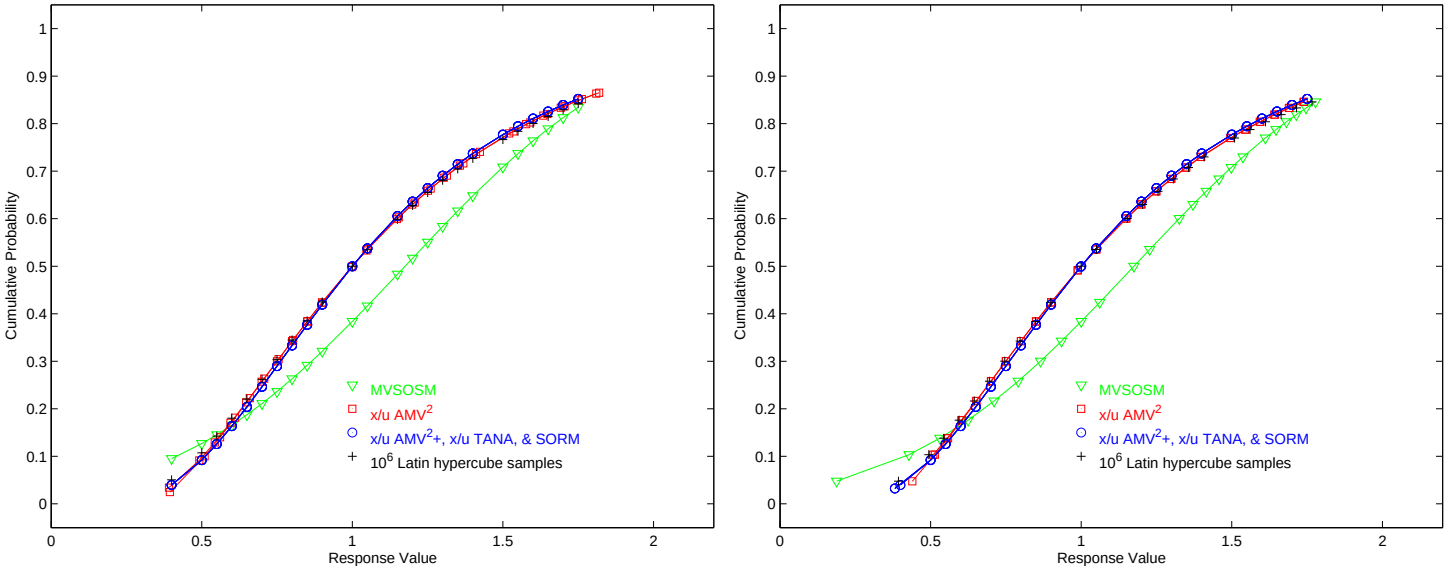

(a) RIA methods (b) PMA methods

Figure 1. Lognormal ratio cumulative distribution function, RIA/PMA methods with analytic Hessians.

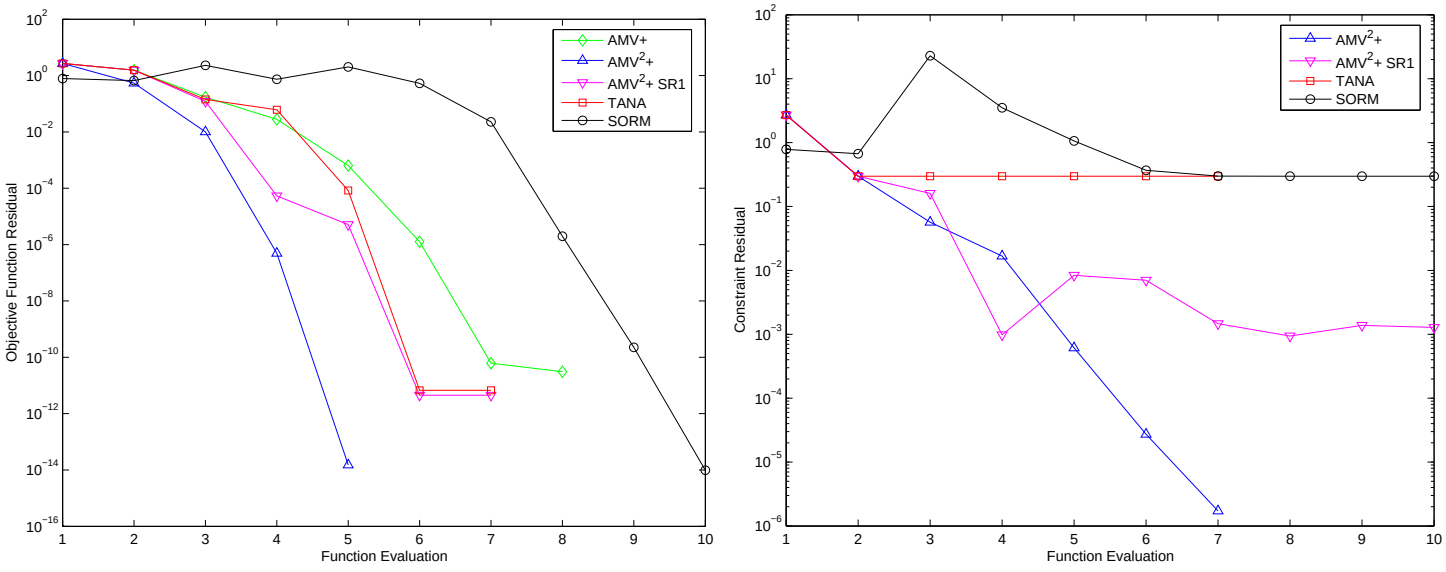

(a) RIA methods ($\bar{z} = 0.4$) (b) PMA methods ($\bar{p} = 0.0396$)

Figure 2. Lognormal ratio MPP convergence rates, x-space methods for first level.

estimate curvature than to retain positive definiteness). For second-order PMA, the AMV^2+ approaches consistently find the correct solution, whereas SORM and TANA approaches have minor convergence difficulties (for the first probability level only). When looking more closely at convergence for the first RIA and PMA levels, Figure 2 shows rates that are quadratic in nature for second-order RIA, but which are more linear in nature for the successful PMA methods due to the $\bar{p} \rightarrow \bar{\beta}$ updates. Quadratic rates (and more consistent convergence) would be expected for PMA with prescribed $\bar{\beta}$ levels. Finally, optimizer selection has a large effect when not employing approximations, and the NIP option can be seen to significantly outperform the SQP option and remain competitive with the approximation-based approaches.

In comparison with first-order method performance presented in Ref. 11, most of the new second-order methods show significant improvement. With the addition of analytic Hessians, AMV^2 shows improved accuracy (e.g., a 5x reduction in RIA z offset error on average) and AMV^2+ shows faster convergence (e.g., a 35% reduction in function evaluations for x-space AMV^2+). More importantly for practical applications, quasi-Newton SR1 x-space AMV^2+ shows a 24% reduction in expense over first-order AMV+ with no additional data requirements.

B. Short column

This test problem involves the plastic analysis and design of a short column with rectangular cross section (width b and depth h) having uncertain material properties (yield stress Y) and subject to uncertain loads (bending moment M and axial force P).[20] The limit state function is defined as:

$$g(\mathbf{x}) = 1 - \frac{4M}{bh^2Y} - \frac{P^2}{b^2h^2Y^2} \tag{55}$$

The distributions for P, M, and Y are Normal(500, 100), Normal(2000, 400), and Lognormal(5, 0.5), respectively, with a correlation coefficient of 0.5 between P and M (uncorrelated otherwise). The nominal values for b and h are 5 and 15, respectively.

1. Uncertainty quantification

For RIA, 43 response levels (-9.0, -8.75, -8.5, -8.0, -7.75, -7.5, -7.25, -7.0, -6.5, -6.0, -5.5, -5.0, -4.5, -4.0, -3.5, -3.0, -2.5, -2.0, -1.9, -1.8, -1.7, -1.6, -1.5, -1.4, -1.3, -1.2, -1.1, -1.0, -0.9, -0.8, -0.7, -0.6, -0.5, -0.4, -0.3, -0.2, -0.1, 0.0, 0.05, 0.1, 0.15, 0.2, 0.25) are mapped into the corresponding cumulative probability levels using first-order (for MVSOSM and AMV^2) or second-order (for AMV^2+, TANA, and SORM) integrations. For PMA, these 43 probability levels (the fully converged first-order or second-order results from RIA FORM/SORM) are mapped back into the original response levels (using updating schemes in the second-order case for $\bar{\beta}(\bar{p})$). Tables 5 and 7 show the computational results for each of the primary RIA and PMA method variants using analytic limit state gradients and Hessians, and Tables 6 and 8 show the computational results for RIA and PMA with AMV^2+ using either numerical Hessians or quasi-Newton Hessian updates. The RIA p error norms and PMA z error norms are measured relative to the corresponding fully-converged FORM or SORM results. That is, the inherent reliability analysis errors (e.g., RIA SORM p error norm of 0.01593 and PMA SORM z error norm of 0.2181) relative to a Latin Hypercube reference solution of 10^6 samples are omitted in order to avoid obscuring the relative errors. Figure 3 overlays the computed CDF values for each of the eight primary method variants corresponding to Tables 5 and 7 as well as the Latin Hypercube reference solution.

Table 5. RIA results for short column problem using analytic Hessians.

RIA Approach	SQP Function Evals (val/grad/Hessian)	NIP Function Evals (val/grad/Hessian)	CDF p Error Norm	Target z Offset Norm
MVSOSM	1 (1/1/1)	1 (1/1/1)	0.1127	0.0
x-space AMV^2	45 (45/1/1)	45 (45/1/1)	0.002063	2.482
u-space AMV^2	45 (45/1/1)	45 (45/1/1)	0.001410	2.031
x-space AMV^2+	125 (125/124/124)	131 (131/130/130)	0.0	0.0
u-space AMV^2+	122 (122/121/121)	130 (130/129/129)	0.0	0.0
x-space TANA	245 (245/244/43)	246 (246/245/43)	0.0	0.0
u-space TANA	296* (296/295/43)	278* (278/277/43)	6.982e-5	0.08014
SORM	669 (626/625/43)	219 (176/175/43))	0.0	0.0

Relative to the fully-converged SORM results, MVSOSM is now reasonably accurate and greatly improved over the lognormal ratio test problem. AMV^2 improves on the MVSOSM results, although with significant offsets in the RIA

Table 6. RIA results for short column problem using numerical Hessians (NH) and quasi-Hessians (QH).

RIA Approach	SQP Function Evals (val/grad/Hessian)	NIP Function Evals (val/grad/Hessian)	CDF p Error Norm	Target z Offset Norm
x-space AMV^2+ NH	481 (121/480/0)	521 (131/520/0)	4.156e-7	4.341e-8
u-space AMV^2+ NH	513 (129/512/0)	517 (130/516/0)	4.195e-7	4.355e-8
x-space AMV^2+ QH SR1	137 (137/136/0)	137 (137/136/0)	4.748e-5	4.372e-8
u-space AMV^2+ QH SR1	139 (139/138/0)	138 (138/137/0)	1.164e-4	4.317e-8
x-space AMV^2+ QH BFGS	290* (290/289/0)	227* (227/226/0)	1.001	12.70
u-space AMV^2+ QH BFGS	294* (294/293/0)	240* (240/239/0)	1.121	13.85

Table 7. PMA results for short column problem using analytic Hessians.

PMA Approach	SQP Function Evals (val/grad/Hessian)	NIP Function Evals (val/grad/Hessian)	CDF z Error Norm	Target p Offset Norm
MVSOSM	1 (1/1/1)	1 (1/1/1)	6.823	0.0
x-space AMV^2	45 (45/1/1)	45 (45/1/1)	2.730	0.0
u-space AMV^2	45 (45/1/1)	45 (45/1/1)	2.828	0.0
x-space AMV^2+	135 (135/134/134)	142 (142/141/141)	0.0	0.0
u-space AMV^2+	132 (132/131/131)	139 (139/138/138)	0.0	0.0
x-space TANA	293* (293/292/43)	272 (272/271/43)	0.04259	1.598e-4
u-space TANA	325* (325/324/43)	311* (311/310/43)	2.208	5.600e-4
SORM	535 (535/534/534)	191* (191/190/190)	2.410	6.522e-4

Table 8. PMA results for short column problem using numerical Hessians (NH) and quasi-Hessians (QH).

PMA Approach	SQP Function Evals (val/grad/Hessian)	NIP Function Evals (val/grad/Hessian)	CDF z Error Norm	Target p Offset Norm
x-space AMV^2+ NH	537 (135/536/0)	565 (142/564/0)	5.020e-6	7.556e-8
u-space AMV^2+ NH	525 (132/524/0)	553 (139/552/0)	4.628e-6	1.101e-7
x-space AMV^2+ QH SR1	255* (255/254/0)	252 (252/251/0)	0.004965	5.924e-5
u-space AMV^2+ QH SR1	252 (252/251/0)	250 (250/249/0)	0.08599	2.093e-4
x-space AMV^2+ QH BFGS	336* (336/335/0)	345* (345/344/0)	0.3979	6.133e-4
u-space AMV^2+ QH BFGS	316* (316/315/0)	342* (342/341/0)	0.2178	0.003301

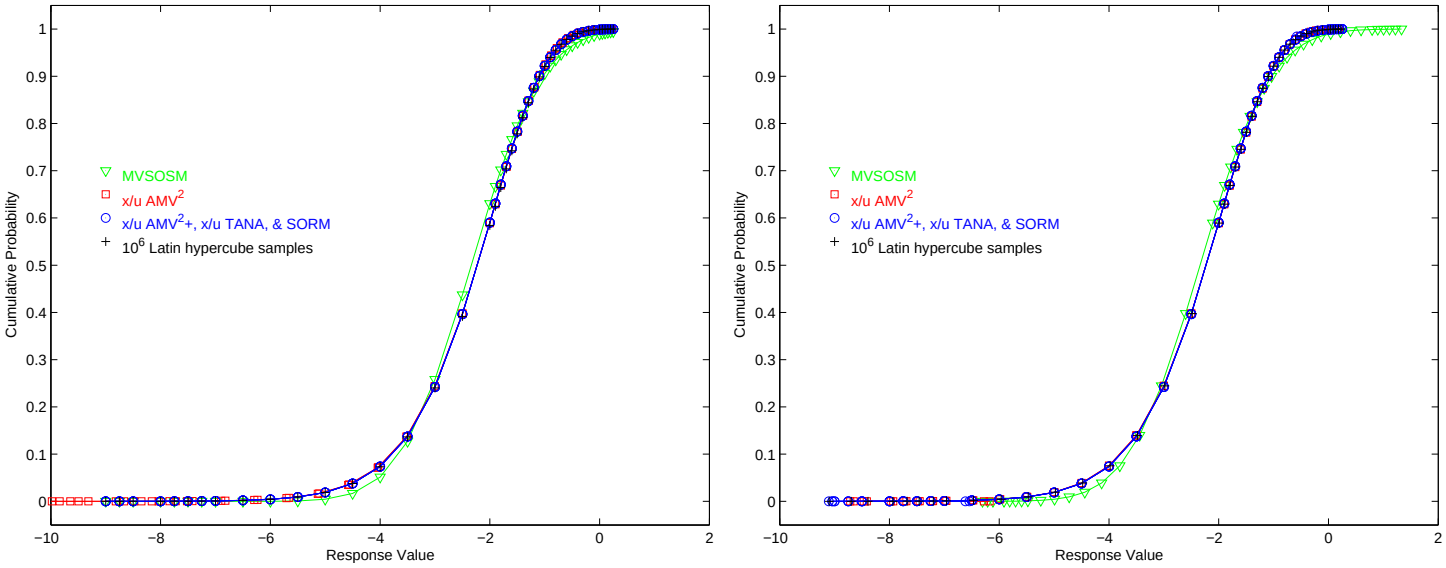

(a) RIA methods

(b) PMA methods

Figure 3. Short column cumulative distribution function, RIA/PMA methods with analytic Hessians.

case from the target response levels. In the RIA case, AMV^2+ and TANA have full accuracy and AMV^2+ with analytic Hessians reduces expense by a factor of 2.1 on average in comparison to TANA and by a factor of 3.5 on average in comparison to SORM. For PMA, AMV^2+ with analytic Hessians is both the most robust and the most efficient approach. For AMV^2+ with approximated Hessians, SR1 updating is again the best approach.

In comparison with first-order AMV+ performance presented in Ref. 11, AMV^2+ for RIA reduces function evaluation counts by 36% with analytic Hessians and by 31% in the quasi-Newton SR1 case, on average. For PMA, where the second-order case is more challenging than the first-order case in converging to a prescribed $\bar{p}$, AMV^2+ reduces function evaluation counts by 27% for PMA with analytic Hessians, but increases function evaluation counts by 34% in the quasi-Newton SR1 case, on average.

2. Reliability-based design optimization

The short column example problem is also amenable to RBDO. An objective function of cross-sectional area and a target reliability index of 2.5 are used in the design problem:

$$\begin{aligned} \min \quad & bh \\ \text{s.t.} \quad & \beta \geq 2.5 \\ & 5.0 \leq b \leq 15.0 \\ & 15.0 \leq h \leq 25.0 \end{aligned} \tag{56}$$

It is important to note that only a single response/probability mapping is needed for each uncertainty analysis (instead of the 43 used previously in generating a full CDF). As is evident from the UQ results shown in Figure 3, the nominal design of $(b, h) = (5, 15)$ is infeasible ($p(g \leq 0) > 0.9$) and the optimization must add material to obtain the target reliability at the optimal design $(b, h) = (8.669, 25.00)$. Eq. 56 corresponds to an RIA $\bar{z} \rightarrow \beta$ approach, whereas an RIA $\bar{z} \rightarrow p$ approach would constrain p and PMA $\bar{\beta} \rightarrow z$ and $\bar{p} \rightarrow z$ approaches would constrain z. The second-order cumulative probability corresponding to the optimal solution (used for level specification in PMA $\bar{p} \rightarrow z$ and for the constraint allowable in RIA $\bar{z} \rightarrow p$) is $p(g \leq 0) = 0.005992$, which is relatively close to the corresponding first-order probability of 0.006210.

Table 9 shows the results for fully-analytic bi-level second-order RBDO employing the gradient expressions for z, β, and p (Eqs. 44-45 and 47). Constraint violations are raw norms (not normalized by allowable). SQP is used for optimization at both levels. In this case, MVSOSM and AMV^2 variants for RIA/PMA RBDO are not allowed, since the sensitivity expressions require a fully-converged MPP. The function evaluation tabulations indicate that AMV^2+-based RBDO significantly outperforms SORM-based RBDO by a factor of 6.2 on average. Applying reliability constraints is more computationally efficient than applying probability constraints in the RIA RBDO formulation of Eq. 42 (expense reduced by a factor of 2.0 on average), since β tends to be more linear and well-scaled than p; however, only the formulations

employing p capture the second-order probability corrections. That is, second-order RBDO with probability constraints is more challenging and expensive, but can be more precise in achieving desired probabilistic performance.

Table 9. Analytic bi-level RBDO results, short column test problem.

RBDO Approach	Function Evals (val/grad/Hessian)	Objective Function	Constraint Violation
RIA $\bar{z} \rightarrow p$ x-space AMV^2+	129 (131/129/111)	217.1	0.0
RIA $\bar{z} \rightarrow p$ u-space AMV^2+	130 (132/130/112)	217.1	0.0
RIA $\bar{z} \rightarrow p$ SORM	1204 (1161/1159/25)	217.1	0.0
RIA $\bar{z} \rightarrow \beta$ x-space AMV^2+	67 (66/67/45)	216.7	0.0
RIA $\bar{z} \rightarrow \beta$ u-space AMV^2+	67 (66/67/45)	216.7	0.0
RIA $\bar{z} \rightarrow \beta$ SORM	601 (591/592/0)	216.7	0.0
PMA $\bar{p} \rightarrow z$ x-space AMV^2+	98 (97/98/84)	216.8	0.0
PMA $\bar{p} \rightarrow z$ u-space AMV^2+	98 (97/98/84)	216.8	0.0
PMA $\bar{p} \rightarrow z$ SORM	306 (292/293/266)	217.2	0.0
PMA $\bar{\beta} \rightarrow z$ x-space AMV^2+	98 (97/98/62)	216.8	0.0
PMA $\bar{\beta} \rightarrow z$ u-space AMV^2+	97 (96/97/63)	216.8	0.0
PMA $\bar{\beta} \rightarrow z$ SORM	329 (315/316/0)	216.8	0.0

Table 10 shows the results for sequential RBDO using a trust-region surrogate-based approach with an initial trust region size of 20%. The surrogates are second-order Taylor-series using the same analytic gradients of z, β, and p in combination with SR1 quasi-Newton Hessian updates. The sequential case is consistently more efficient than the fully-analytic bi-level case, with expense reduced by 31% on average for this default initial trust region case. With tuning of the initial trust region, an initial size of 80% solves the problem in as few as 35 function evaluations. Relative to first-order sequential RBDO performance presented in Ref. 11, second-order approaches (analytic second-order Taylor-series at the reliability level and quasi-Newton second-order Taylor-series at the design level) save 8.7% on average and can be more precise.

Table 10. Surrogate-based RBDO results, short column test problem.

RBDO Approach	Function Evals (val/grad/Hessian)	Objective Function	Constraint Violation
RIA $\bar{z} \rightarrow p$ x-space AMV^2+	86 (75/86/64)	218.7	0.0
RIA $\bar{z} \rightarrow p$ u-space AMV^2+	94 (82/94/70)	216.3	2.168e-4
RIA $\bar{z} \rightarrow p$ SORM	718 (670/681/26)	216.5	1.110e-4
RIA $\bar{z} \rightarrow \beta$ x-space AMV^2+	51 (45/51/30)	216.7	0.0
RIA $\bar{z} \rightarrow \beta$ u-space AMV^2+	58 (51/58/34)	216.7	0.0
RIA $\bar{z} \rightarrow \beta$ SORM	560 (545/554/0)	216.7	0.0
PMA $\bar{p} \rightarrow z$ x-space AMV^2+	58 (50/58/44)	216.8	0.0
PMA $\bar{p} \rightarrow z$ u-space AMV^2+	55 (48/55/42)	216.8	0.0
PMA $\bar{p} \rightarrow z$ SORM	128 (116/122/104)	217.2	0.0
PMA $\bar{\beta} \rightarrow z$ x-space AMV^2+	79 (68/79/40)	216.8	0.0
PMA $\bar{\beta} \rightarrow z$ u-space AMV^2+	79 (68/79/40)	216.8	0.0
PMA $\bar{\beta} \rightarrow z$ SORM	171 (159/165/0)	216.8	0.0

C. Cantilever beam

The next test problem involves the simple uniform cantilever beam[26,33] shown in Figure 4.

Random variables in the problem include the yield stress R of the beam material, the Young's modulus E of the material, and the horizontal and vertical loads, X and Y, which are modeled with normal distributions using N(40000,

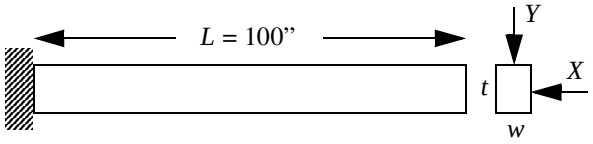

Figure 4. Cantilever beam test problem.

2000), N(2.9E7, 1.45E6), N(500, 100), and N(1000, 100), respectively. Problem constants include $L = 100$ in. and $D_0 = 2.2535$ in. The constraints on beam response have the following analytic form:

$$stress = \frac{600}{wt^2}Y + \frac{600}{w^2t}X \leq R \tag{57}$$

$$displacement = \frac{4L^3}{Ewt}\sqrt{(\frac{Y}{t^2})^2 + (\frac{X}{w^2})^2} \leq D_0 \tag{58}$$

or when scaled:

$$g_S = \frac{stress}{R} - 1 \leq 0 \tag{59}$$

$$g_D = \frac{displacement}{D_0} - 1 \leq 0 \tag{60}$$

1. Uncertainty quantification

For RIA, 11 levels (0.0 to 1.0 in 0.1 increments) are employed for each limit state function (g_S and g_D) and are mapped into the corresponding cumulative probability levels using first-order (for MVSOSM and AMV^2) or second-order (for AMV^2+, TANA, and SORM) integrations. For PMA, these probability levels (the fully converged first-order or second-order results from RIA FORM/SORM) are mapped back into the original response levels (using updating schemes in the second-order case for $\bar{\beta}(\bar{p})$). Tables 11 and 13 show the computational results for each of the primary RIA and PMA method variants using analytic gradients and Hessians, and Tables 12 and 14 show the computational results for RIA and PMA with AMV^2+ using either numerical Hessians or quasi-Newton Hessian updates. In this problem, since all uncertain variables are normally distributed and uncorrelated, the x-space and u-space linearization approaches are equivalent. The RIA p error norms and PMA z error norms are measured relative to the corresponding fully-converged FORM or SORM results. That is, the inherent reliability analysis errors (e.g., RIA SORM p error norm of 0.02943 and PMA SORM z error norm of 0.04198) relative to a Latin Hypercube reference solution of 10^6 samples are not included in order to avoid obscuring the relative errors. Figure 5 overlays the computed CDF values for each of the method variants as well as the Latin Hypercube reference solution (any unconverged CDF values as denoted by $*$ in the tables are omitted for clarity).

Table 11. RIA results for cantilever problem using analytic Hessians.

RIA Approach	SQP Function Evals (val/grad/Hessian)	NIP Function Evals (val/grad/Hessian)	CDF p Error Norm	Target z Offset Norm
MVSOSM	1 (2/2/2)	1 (2/2/2)	0.04064	0.0
x-/u-space AMV^2	23 (24/2/2)	23 (24/2/2)	8.763e-6	0.007661
x-/u-space AMV^2+	59 (60/60/60)	67 (68/68/68)	0.0	0.0
x-/u-space TANA	116 (117/117/22)	123 (124/124/22)	0.0	0.0
SORM	187 (166/164/22)	117 (96/94/22)	0.0	0.0

Relative to the fully-converged SORM results, MVSOSM and AMV^2 are quite accurate for this problem. In the RIA case, AMV^2+ and TANA have full accuracy and AMV^2+ with analytic Hessians outperforms TANA and SORM (reduces function evaluations by factors of 1.9 and 2.5, respectively). For PMA, AMV^2+ with analytic Hessians is again the most robust and efficient approach. For AMV^2+ with approximated Hessians, SR1 updating is again the best approach.

In comparison with first-order AMV+ performance presented in Ref. 11, AMV^2+ for RIA reduces function evaluation counts by 31% with analytic Hessians and by 16% in the quasi-Newton SR1 case, on average. For PMA, where converging to a prescribed second-order $\bar{p}$ is more challenging than the first-order case, AMV^2+ reduces function evaluation counts

Table 12. RIA results for cantilever problem using numerical Hessians (NH) and quasi-Hessians (QH).

RIA Approach	SQP Function Evals (val/grad/Hessian)	NIP Function Evals (val/grad/Hessian)	CDF p Error Norm	Target z Offset Norm
x-/u-space AMV^2+ NH	270 (55/275/0)	335 (68/340/0)	1.202e-7	1.662e-7
x-/u-space AMV^2+ QH SR1	75 (76/76/0)	78 (79/79/0)	0.001014	3.070e-6
x-/u-space AMV^2+ QH BFGS	114 (115/115/0)	107* (108/108/0)	1.145	1.011

Table 13. PMA results for cantilever problem using analytic Hessians.

PMA Approach	SQP Function Evals (val/grad/Hessian)	NIP Function Evals (val/grad/Hessian)	CDF z Error Norm	Target p Offset Norm
MVSOSM	1 (2/2/2)	1 (2/2/2)	0.1025	0.0
x-/u-space AMV^2	23 (24/2/2)	23 (24/2/2)	0.4044	0.006347
x-/u-space AMV^2+	68 (69/69/69)	71 (72/72/72)	0.0	0.0
x-/u-space TANA	118 (119/119/22)	115 (116/116/22)	0.003029	4.137e-4
SORM	248* (249/247/247)	150* (151/149/149)	0.4176	0.006159

Table 14. PMA results for cantilever problem using numerical Hessians (NH) and quasi-Hessians (QH).

PMA Approach	SQP Function Evals (val/grad/Hessian)	NIP Function Evals (val/grad/Hessian)	CDF z Error Norm	Target p Offset Norm
x-/u-space AMV^2+ NH	340 (69/345/0)	355 (72/360/0)	2.152e-7	1.806e-8
x-/u-space AMV^2+ QH SR1	102 (103/103/0)	108 (109/109/0)	0.01348	0.005450
x-/u-space AMV^2+ QH BFGS	159* (160/160/0)	156* (157/157/0)	10.657	0.5833

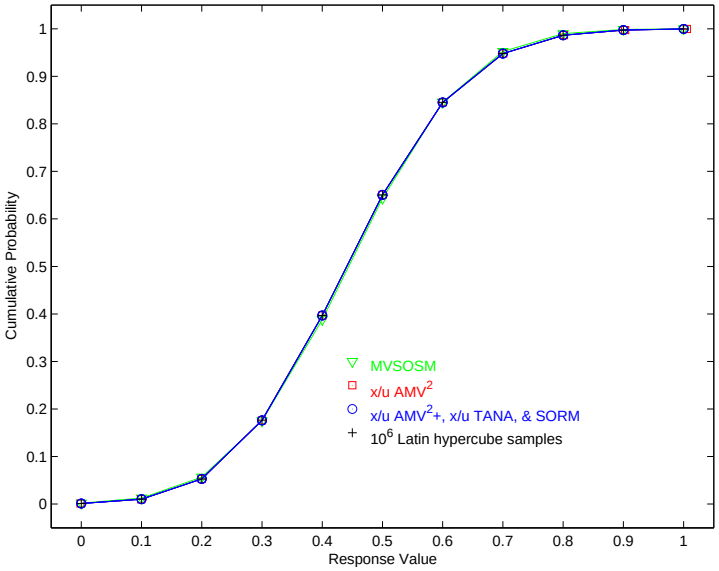

(a) RIA methods, g_S

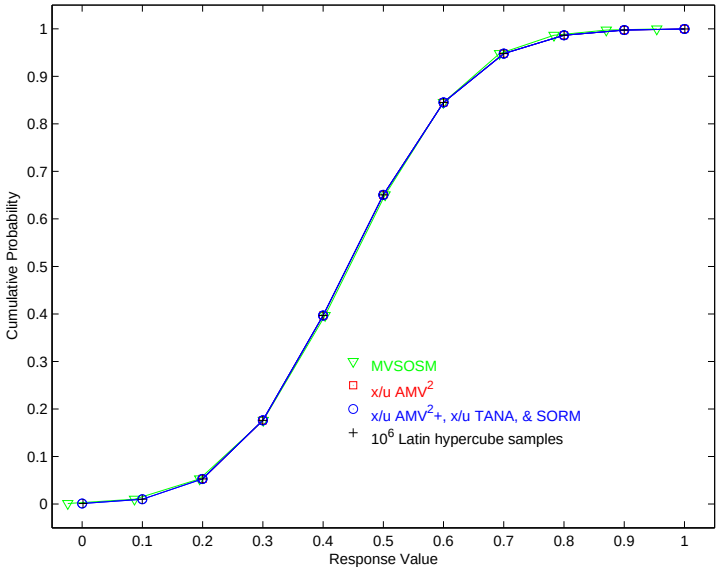

(b) PMA methods, g_S

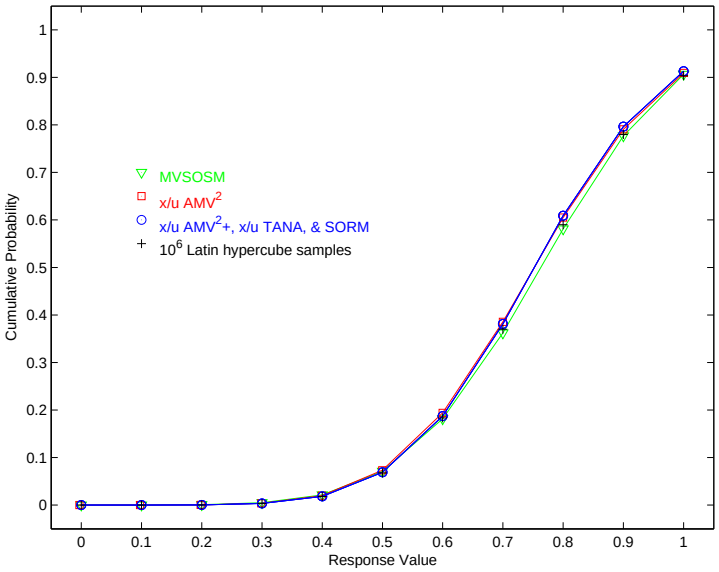

(c) RIA methods, g_D

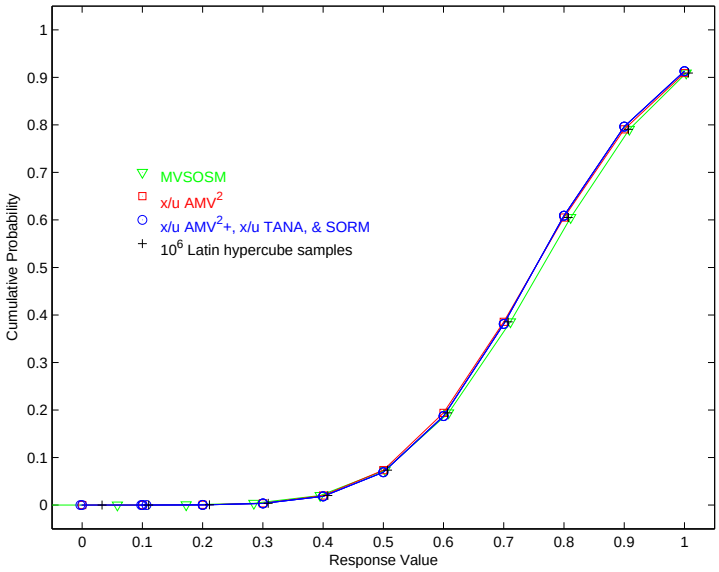

(d) PMA methods, g_D

Figure 5. Cantilever beam cumulative distribution functions, analytic Hessians.

by 10% for PMA with analytic Hessians, but increases function evaluation counts by 35% in the quasi-Newton SR1 case, on average.

2. Reliability-based design optimization

The design problem is to minimize the weight (or, equivalently, the cross-sectional area) of the beam subject to the displacement and stress constraints. If the random variables are fixed at their means, the resulting deterministic design problem (with constraints $g_S \leq 0$ and $g_D \leq 0$) has the solution $(w, t) = (2.352, 3.326)$ with an objective function of 7.824. When seeking reliability levels of 3.0 for these constraints, the design problem becomes:

$$\begin{aligned} \min \quad & wt \\ \text{s.t.} \quad & \beta_D \geq 3.0 \\ & \beta_S \geq 3.0 \\ & 1.0 \leq w \leq 4.0 \\ & 1.0 \leq t \leq 4.0 \end{aligned} \tag{61}$$

which has the solution $(w, t) = (2.451, 3.884)$ with an objective function of 9.520. This formulation corresponds to an RIA $\bar{z} \rightarrow \beta$ approach, whereas an RIA $\bar{z} \rightarrow p$ approach would constrain p and PMA $\bar{\beta} \rightarrow z$ and $\bar{p} \rightarrow z$ approaches would constrain z. The second-order complementary cumulative probabilities corresponding to the optimal solution (used for level specification in PMA $\bar{p} \rightarrow z$ and for the constraint allowable in RIA $\bar{z} \rightarrow p$) are $p(g_S > 0) = 0.001350$ and $p(g_D > 0) = 0.001145$, which are equal and similar, respectively, to the corresponding first-order probabilities of 0.001350.

Table 15 shows the results for fully-analytic bi-level second-order RBDO employing the gradient expressions for z, β, and p (Eqs. 44-45 and 47). Constraint violations are raw norms (not normalized by allowable), and SQP is used for optimization at both levels. AMV^2+-based RBDO reduces expense relative to SORM-based RBDO by a factor of 2.9 on average. β-based formulations are again more computationally efficient, but lack the precision of second-order probability integrations.

Table 15. Analytic bi-level RBDO results, cantilever test problem.

RBDO Approach	Function Evals (val/grad/Hessian)	Objective Function	Constraint Violation
RIA $\bar{z} \rightarrow p$ x-/u-space AMV^2+	258 (279/312/279)	9.562	0.0
RIA $\bar{z} \rightarrow p$ SORM	625 (551/530/58)	9.562	0.0
RIA $\bar{z} \rightarrow \beta$ x-/u-space AMV^2+	183 (189/213/143)	9.520	0.0
RIA $\bar{z} \rightarrow \beta$ SORM	335 (326/320/0)	9.520	0.0
PMA $\bar{p} \rightarrow z$ x-/u-space AMV^2+	262 (278/302/278)	9.519	2.245e-4
PMA $\bar{p} \rightarrow z$ SORM	853 (849/833/789)	9.519	2.027e-4
PMA $\bar{\beta} \rightarrow z$ x-/u-space AMV^2+	208 (224/248/174)	9.521	0.0
PMA $\bar{\beta} \rightarrow z$ SORM	855 (851/835/0)	9.521	0.0

Table 16 shows the results for sequential RBDO using a trust-region surrogate-based approach with an initial trust region size of 20%. The surrogates are again second-order Taylor-series using analytic gradients of z, β, and p in combination with SR1 quasi-Newton Hessian updates. The sequential case is more efficient than the fully-analytic bi-level case, with expense reduced by 41% on average. With tuning of the initial trust region, an initial size of 10% solves the problem in as few as 75 function evaluations. Relative to first-order sequential RBDO performance presented in Ref. 11, second-order approaches (analytic second-order Taylor-series at the reliability level and quasi-Newton second-order Taylor-series at the design level) save 29% on average and can be more precise.

D. Steel Column

The final test problem involves the trade-off between cost and reliability for a steel column.[20] The cost is defined as

$$Cost = bd + 5h \tag{62}$$

where b, d, and h are the means of the flange breadth, flange thickness, and profile height, respectively. Nine uncorrelated random variables are used in the problem to define the yield stress F_s (lognormal with $\mu/\sigma = 400/35$ MPa), dead weight

Table 16. Surrogate-based RBDO results, cantilever test problem.

RBDO Approach	Function Evals (val/grad/Hessian)	Objective Function	Constraint Violation
RIA $\bar{z} \rightarrow p$ x-/u-space AMV^2+	174 (163/202/163)	9.618	0.0
RIA $\bar{z} \rightarrow p$ SORM	324 (265/274/38)	9.534	2.570e-5
RIA $\bar{z} \rightarrow \beta$ x-/u-space AMV^2+	118 (110/134/83)	9.521	0.0
RIA $\bar{z} \rightarrow \beta$ SORM	213 (198/205/0)	9.521	0.0
PMA $\bar{p} \rightarrow z$ x-/u-space AMV^2+	134 (125/148/125)	9.521	0.0
PMA $\bar{p} \rightarrow z$ SORM	515 (501/508/480)	9.521	0.0
PMA $\bar{\beta} \rightarrow z$ x-/u-space AMV^2+	102 (95/116/69)	9.522	2.525e-3
PMA $\bar{\beta} \rightarrow z$ SORM	558 (549/549/0)	9.522	0.0

load P_1 (normal with $\mu/\sigma = 500000/50000$ N), variable load P_2 (gumbel with $\mu/\sigma = 600000/90000$ N), variable load P_3 (gumbel with $\mu/\sigma = 600000/90000$ N), flange breadth B (lognormal with $\mu/\sigma = b/3$ mm), flange thickness D (lognormal with $\mu/\sigma = d/2$ mm), profile height H (lognormal with $\mu/\sigma = h/5$ mm), initial deflection F_0 (normal with $\mu/\sigma = 30/10$ mm), and youngs modulus E (weibull with $\mu/\sigma = 21000/4200$ MPa). The limit state has the following analytic form:

$$g = F_s - P\left(\frac{1}{2BD} + \frac{F_0}{BDH}\frac{E_b}{E_b - P}\right) \tag{63}$$

where

$$P = P_1 + P_2 + P_3 \tag{64}$$

$$E_b = \frac{\pi^2 EBDH^2}{2L^2} \tag{65}$$

and the column length L is 7500 mm.

1. Reliability-based design optimization

This design problem demonstrates design variable insertion into random variable distribution parameters through the design of the mean flange breadth, flange thickness, and profile height. The following RBDO formulation maximizes the reliability subject to a cost constraint:

$$\begin{aligned} \max \quad & \beta \\ \text{s.t.} \quad & Cost \leq 4000. \\ & 200.0 \leq b \leq 400.0 \\ & 10.0 \leq d \leq 30.0 \\ & 100.0 \leq h \leq 500.0 \end{aligned} \tag{66}$$

which has the solution (b, d, h) = (200.0, 17.50, 100.0) with a maximal reliability of 3.132. This corresponds to an RIA $\bar{z} \rightarrow \beta$ approach, where the RIA $\bar{z} \rightarrow p$ approach would minimize p and the PMA $\bar{\beta} \rightarrow z$ and $\bar{p} \rightarrow z$ approaches would maximize z. The second-order cumulative probability corresponding to the optimal solution (used for PMA $\bar{p} \rightarrow z$) is $p(g \leq 0) = 0.001309$, which differs significantly from the corresponding first-order probability of 8.678e-4.

Table 17 shows the results for fully-analytic bi-level second-order RBDO employing the gradient expressions for z, β, and p (Eqs. 47-51). Constraint violations are raw norms (not normalized by allowable), and SQP and NIP are used for optimization at the design and MPP search levels, respectively. With the use of NIP at the reliability level, the benefits of AMV^2+-based RBDO relative to SORM-based RBDO are less pronounced, with average reductions in expense of 17% on average. β-based formulations are again more computationally efficient (although less precise with the omission of second-order probability integrations) and are also more robust since second-order PMA with $\bar{p}$ had some difficulty: while it located the correct optimal solution, the final response level (marked with "*") was incorrect due to inaccurate $\bar{p} \rightarrow \bar{\beta}$ inversions.

Table 18 shows the results for sequential RBDO using a trust-region surrogate-based approach with an initial trust region size of 20%. The surrogates are second-order Taylor-series using analytic gradients of z, β, and p in combination

Table 17. Analytic bi-level RBDO results, steel column test problem.

RBDO Approach	Function Evals (val/grad/Hessian)	Objective Function	Constraint Violation
RIA $\bar{z} \rightarrow p$ x-space AMV^2+	315 (315/272/229)	0.001309	0.0
RIA $\bar{z} \rightarrow p$ u-space AMV^2+	311 (311/268/225)	0.001309	0.0
RIA $\bar{z} \rightarrow p$ SORM	322 (279/236/43)	0.001309	0.0
RIA $\bar{z} \rightarrow \beta$ x-space AMV^2+	90 (90/78/54)	3.132	0.0
RIA $\bar{z} \rightarrow \beta$ u-space AMV^2+	88 (88/76/52)	3.132	0.0
RIA $\bar{z} \rightarrow \beta$ SORM	90 (90/78/0)	3.132	0.0
PMA $\bar{p} \rightarrow z$ x-space AMV^2+	52 (52/45/38)	0.001481	0.0
PMA $\bar{p} \rightarrow z$ u-space AMV^2+	53 (53/46/39)	0.001481	0.0
PMA $\bar{p} \rightarrow z$ SORM	67 (67/60/53)	7.401*	0.0
PMA $\bar{\beta} \rightarrow z$ x-space AMV^2+	49 (49/42/28)	0.005223	0.0
PMA $\bar{\beta} \rightarrow z$ u-space AMV^2+	48 (48/41/27)	0.005223	0.0
PMA $\bar{\beta} \rightarrow z$ SORM	83 (83/76/0)	0.005221	0.0

with SR1 quasi-Newton Hessian updates. The sequential and bi-level cases are more competitive in this problem, but sequential is still more efficient with expense reduced by 13% on average. Second-order PMA with $\bar{p}$ again had difficulty. With tuning of the initial trust region, an initial size of 80% solves the problem in as few as 45 function evaluations.

Table 18. Surrogate-based RBDO results, steel column test problem.

RBDO Approach	Function Evals (val/grad/Hessian)	Objective Function	Constraint Violation
RIA $\bar{z} \rightarrow p$ x-space AMV^2+	62 (62/49/44)	0.001309	0.0
RIA $\bar{z} \rightarrow p$ u-space AMV^2+	62 (62/49/44)	0.001309	0.0
RIA $\bar{z} \rightarrow p$ SORM	81 (72/59/9)	0.001309	0.0
RIA $\bar{z} \rightarrow \beta$ x-space AMV^2+	67 (67/52/37)	3.132	0.0
RIA $\bar{z} \rightarrow \beta$ u-space AMV^2+	67 (67/52/37)	3.132	0.0
RIA $\bar{z} \rightarrow \beta$ SORM	78 (78/63/0)	3.132	0.0
PMA $\bar{p} \rightarrow z$ x-space AMV^2+	64 (64/49/44)	0.001500	0.0
PMA $\bar{p} \rightarrow z$ u-space AMV^2+	63 (63/48/43)	0.001500	0.0
PMA $\bar{p} \rightarrow z$ SORM	86 (86/71/66)	7.401*	0.0
PMA $\bar{\beta} \rightarrow z$ x-space AMV^2+	62 (62/47/32)	0.005223	0.0
PMA $\bar{\beta} \rightarrow z$ u-space AMV^2+	60 (60/45/30)	0.005223	0.0
PMA $\bar{\beta} \rightarrow z$ SORM	102 (102/87/0)	0.005223	0.0

V. Conclusions

The effectiveness of first-order approximations, both in limit state linearization within reliability analysis and in surrogate-based RBDO, has led to additional work in second-order approximations which seek improved accuracy in probability integrations and improved computational efficiency through accelerated convergence rates.

This paper explores second-order RIA and PMA formulations using various limit state approximation (MVSOSM, x-/u-space AMV^2, x-/u-space AMV^2+, x-/u-space TANA, and SORM), probability integration (first-order or second-order), Hessian approximation (finite difference, BFGS, or SR1), and MPP optimization algorithm (SQP or NIP) selections. When performing the $\bar{p} \rightarrow z$ PMA mapping, an updating scheme for $\bar{\beta}$ is used to account for changes in the limit state curvature.

Reliability analysis results for the lognormal ratio, short column, and cantilever test problems indicate several trends.

MVSOSM and AMV^2 are significantly less expensive than AMV^2+, TANA, and SORM, but come with corresponding reductions in accuracy. In combination, these methods provide a useful spectrum of accuracy and expense that allow the computational effort to be balanced with the precision desired for particular applications. In addition, support for forward and inverse mappings (RIA and PMA) provide the flexibility to support different UQ analysis needs. The AMV^2+ approaches were shown to be the most efficient for second-order RIA analysis and both the most robust and the most efficient for second-order PMA analysis with prescribed probability levels. Analytic Hessians were highly effective in AMV^2+, but since they are often unavailable in practical applications, finite-difference numerical Hessians and quasi-Newton Hessian approximations were also demonstrated, with SR1 quasi-Newton updates being shown to be sufficiently accurate and competitive with analytic Hessian performance. Relative to first-order AMV+ performance, AMV^2+ with analytic Hessians had consistently superior efficiency, and AMV^2+ with quasi-Newton Hessians had improved performance in most cases (it was more expensive than AMV+ only when a more challenging second-order $\bar{p}$ problem was being solved).

An important question is how Taylor-series based limit state approximations (such as AMV+ and AMV^2+) can frequently outperform the best general-purpose optimizers (such as SQP and NIP). The answer likely lies in the exploitation of the structure of the RIA and PMA MPP problems. By approximating the limit state but retaining $\mathbf{u}^T\mathbf{u}$ explicitly, specific problem structure knowledge is utilized in formulating a mixed surrogate/direct approach.

These reliability analysis capabilities provide a substantial foundation for RBDO formulations, and bi-level and sequential RBDO approaches have been investigated. Both approaches have utilized analytic gradients for z, β, and second-order p with respect to augmented and inserted design variables, and sequential RBDO has additionally utilized a trust-region surrogate-based approach to manage the extent of the second-order Taylor-series approximations.

RBDO results for the short column, cantilever, and steel column test problems build on the reliability analysis trends. In bi-level and sequential RBDO, the AMV^2+ approaches were consistently more efficient than the SORM-based approaches. In addition, sequential RBDO approaches demonstrated computational savings over the corresponding bi-level RBDO approaches. The combination of sequential RBDO using AMV^2+ was the most effective of all of the approaches. With initial trust region size tuning, RBDO computational expense for these test problems was shown to be as low as approximately 40 function evaluations per limit state (35 for a single limit state in short column, 75 for two limit states in cantilever, and 45 for a single limit state in steel column). Second-order RBDO with probability constraints was shown to be more challenging and expensive, but could be more precise in achieving the desired probabilistic performance.

Overall, second-order reliability analysis and design approaches appear to serve multiple synergistic needs. The same Hessian information that allows for more accurate probability integrations can also be applied to making MPP solutions more efficient and more robust. Conversely, limit state curvature information accumulated during an MPP search can be reused to improve the accuracy of probability estimates. Future algorithmic directions include sequential RBDO with mixed surrogate and direct models (for probabilistic and deterministic components, respectively). Initial deployment of these algorithmic capabilities within Sandia labs is targeting probabilistic analysis and design of micro-electro-mechanical systems (MEMS).

VI. Acknowledgments

The authors would like to express their thanks to the Sandia Computer Science Research Institute (CSRI) for support of this collaborative work between Sandia National Laboratories and Vanderbilt University.

References

[1]Adams, B.M., Eldred, M.S., Wittwer, J.W., and Massad, J.E., Reliability-Based Design Optimization for Shape Design of Compliant Micro-Electro-Mechanical Systems, to appear in *Proceedings of the 11th AIAA/ISSMO Multidisciplinary Analysis and Optimization Conference*, Portsmouth, VA, Sept. 6-8, 2006.

[2]Agarwal, H., Renaud, J.E., Lee, J.C., and Watson, L.T., A Unilevel Method for Reliability Based Design Optimization, paper AIAA-2004-2029 in *Proceedings of the 45th AIAA/ASME/ASCE/AHS/ASC Structures, Structural Dynamics, and Materials Conference*, Palm Springs, CA, April 19-22, 2004.

[3]Allen, M. and Maute, K., Reliability-based design optimization of aeroelastic structures, *Struct. Multidiscip. O.*, Vol. 27, 2004, pp. 228-242.

[4]Box, G.E.P. and Cox, D.R., An Analysis of Transformations, *J. Royal Stat. Soc.*, Series B, Vol. 26, 1964, pp. 211-252.

[5]Breitung, K., Asymptotic approximation for multinormal integrals, *J. Eng. Mech., ASCE*, Vol. 110, No. 3, 1984, pp. 357-366.

[6]Chen, X., and Lind, N.C., Fast Probability Integration by Three-Parameter Normal Tail Approximation, *Struct. Saf.*, Vol. 1, 1983, pp. 269-276.

[7]Der Kiureghian, A. and Liu, P.L., Structural Reliability Under Incomplete Probability Information, *J. Eng. Mech., ASCE*, Vol. 112, No. 1, 1986, pp. 85-104.

[8]Du, X. and Chen, W., Sequential Optimization and Reliability Assessment Method for Efficient Probabilistic Design, *J. Mech. Design*, Vol. 126, 2004, pp.225-233.

[9]Eldred, M.S., Giunta, A.A., Wojtkiewicz, S.F., Jr., and Trucano, T.G., Formulations for Surrogate-Based Optimization Under Uncertainty,

paper AIAA-2002-5585 in *Proceedings of the 9th AIAA/ISSMO Symposium on Multidisciplinary Analysis and Optimization*, Atlanta, GA, Sept. 4-6, 2002.

[10]Eldred, M.S., Giunta, A.A., van Bloemen Waanders, B.G., Wojtkiewicz, S.F., Jr., Hart, W.E., and Alleva, M.P., DAKOTA, A Multilevel Parallel Object-Oriented Framework for Design Optimization, Parameter Estimation, Uncertainty Quantification, and Sensitivity Analysis. Version 3.1 Users Manual. Sandia Technical Report SAND2001-3796, Revised April 2003, Sandia National Laboratories, Albuquerque, NM.

[11]Eldred, M.S., Agarwal, H., Perez, V.M., Wojtkiewicz, S.F., Jr., and Renaud, J.E., Investigation of Reliability Method Formulations in DAKOTA/UQ, (to appear) *Structure & Infrastructure Engineering: Maintenance, Management, Life-Cycle Design & Performance*, Taylor & Francis Group.

[12]Fadel, G.M., Riley, M.F., and Barthelemy, J.-F.M., Two Point Exponential Approximation Method for Structural Optimization, *Structural Optimization*, Vol. 2, No. 2, 1990, pp. 117-124.

[13]Gill, P.E., Murray, W., Saunders, M.A., and Wright, M.H., User's Guide for NPSOL 5.0: A Fortran Package for Nonlinear Programming, System Optimization Laboratory, Technical Report SOL 86-1, Revised July 1998, Stanford University, Stanford, CA.

[14]Giunta, A.A. and Eldred, M.S., Implementation of a Trust Region Model Management Strategy in the DAKOTA Optimization Toolkit, paper AIAA-2000-4935 in *Proceedings of the 8th AIAA/USAF/NASA/ISSMO Symposium on Multidisciplinary Analysis and Optimization*, Long Beach, CA, September 6-8, 2000.

[15]Haldar, A. and Mahadevan, S., Probability, Reliability, and Statistical Methods in Engineering Design, 2000 (Wiley: New York).

[16]Hohenbichler, M. and Rackwitz, R., Sensitivity and importance measures in structural reliability, *Civil Eng. Syst.*, Vol. 3, 1986, pp. 203-209.

[17]Hohenbichler, M. and Rackwitz, R., Improvement of second-order reliability estimates by importance sampling, *J. Eng. Mech., ASCE*, Vol. 114, No. 12, 1988, pp. 2195-2199.

[18]Hong, H.P., Simple Approximations for Improving Second-Order Reliability Estimates, *J. Eng. Mech., ASCE*, Vol. 125, No. 5, 1999, pp. 592-595.

[19]Karamchandani, A. and Cornell, C.A., Sensitivity estimation within first and second order reliability methods, *Struct. Saf.*, Vol. 11, 1992, pp. 95-107.

[20]Kuschel, N. and Rackwitz, R., Two Basic Problems in Reliability-Based Structural Optimization, *Math. Method Oper. Res.*, Vol. 46, 1997, pp.309-333.

[21]Meza, J.C., OPT++: An Object-Oriented Class Library for Nonlinear Optimization, Sandia Technical Report SAND94-8225, Sandia National Laboratories, Livermore, CA, March 1994.

[22]Nocedal, J., and Wright, S.J., Numerical Optimization, Springer, New York, 1999.

[23]Rackwitz, R., and Fiessler, B., Structural Reliability under Combined Random Load Sequences, *Comput. Struct.*, Vol. 9, 1978, pp. 489-494.

[24]Rackwitz, R., Optimization and risk acceptability based on the Life Quality Index, *Struct. Saf.*, Vol. 24, 2002, pp. 297-331.

[25]Rosenblatt, M., Remarks on a Multivariate Transformation, *Ann. Math. Stat.*, Vol. 23, No. 3, 1952, pp. 470-472.

[26]Sues, R., Aminpour, M. and Shin, Y., Reliability-Based Multidisciplinary Optimization for Aerospace Systems, paper AIAA-2001-1521 in *Proceedings of the 42rd AIAA/ASME/ASCE/AHS/ASC Structures, Structural Dynamics, and Materials Conference*, Seattle, WA, April 16-19, 2001.

[27]Tu, J., Choi, K.K., and Park, Y.H., A New Study on Reliability-Based Design Optimization, *J. Mech. Design*, Vol. 121, 1999, pp.557-564.

[28]Wang, L. and Grandhi, R.V., Efficient Safety Index Calculation for Structural Reliability Analysis, *Comput. Struct.*, Vol. 52, No. 1, 1994, pp. 103-111.

[29]Wojtkiewicz, S.F., Jr., Eldred, M.S., Field, R.V., Jr., Urbina, A., and Red-Horse, J.R., A Toolkit For Uncertainty Quantification In Large Computational Engineering Models, paper AIAA-2001-1455 in *Proceedings of the 42nd AIAA/ASME/ASCE/AHS/ASC Structures, Structural Dynamics, and Materials Conference*, Seattle, WA, April 16-19, 2001.

[30]Wu, Y.-T., and Wirsching, P.H., A new algorithm for structural reliability estimation, *J. Eng. Mech., ASCE*, Vol. 113, 1987, pp. 1319-1336.

[31]Wu, Y.-T., Millwater, H.R., and Cruse, T.A., Advanced Probabilistic Structural Analysis Method for Implicit Performance Functions, *AIAA J.*, Vol. 28, No. 9, 1990, pp. 1663-1669.

[32]Wu, Y.-T., Computational Methods for Efficient Structural Reliability and Reliability Sensitivity Analysis, *AIAA J.*, Vol. 32, No. 8, 1994, pp. 1717-1723.

[33]Wu, Y.-T., Shin, Y., Sues, R., and Cesare, M., Safety-Factor Based Approach for Probability-Based Design Optimization, paper AIAA-2001-1522 in *Proceedings of the 42rd AIAA/ASME/ASCE/AHS/ASC Structures, Structural Dynamics, and Materials Conference*, Seattle, WA, April 16-19, 2001.

[34]Xu, S., and Grandhi, R.V., Effective Two-Point Function Approximation for Design Optimization, *AIAA J.*, Vol. 36, No. 12, 1998, pp. 2269-2275.

[35]Zou, T., Mahadevan, S., and Rebba, R., Computational Efficiency in Reliability-Based Optimization, *Proceedings of the 9th ASCE Specialty Conference on Probabilistic Mechanics and Structural Reliability*, Albuquerque, NM, July 26-28, 2004.